LSPSM/inversion for pre- and poststack time lapse studies

Abdolnaser Yousefzadeh and John C. Bancroft

ABSTRACT

The ability of separate and joint LSPSM/inversion of time lapse data is shown. Assuming similarity of the acquisition instruments, environmental noise, near surface effects, and processing flows and parameters for both, baseline and monitor surveys, difference in acquisition geometries leaves different artifacts at the migration images. It is shown how separate LSPSM of both, baseline and monitor, datasets can attenuate acquisition footprints and create reliable time lapse images. The reconstructed data from two surveys makes the prestack time lapse studies more feasible. Formulations of the joint inversion of time lapse data to invert for the baseline image and time lapse image by LSCG method are derived.

INTRODUCTION

Time lapse or 4D (time as the fourth dimension) study of seismic data includes recording and analysing a secondary seismic survey after a period of time in order to detect the subtle changes in the physical properties of the hydrocarbon reservoirs. These changes can be due to either production or injection of a fluid (oil, gas, water, steam, etc.) from or into the reservoirs.

Usually, the first seismic survey is called baseline survey and later ones are called monitor surveys. Assuming all acquisition parameters, instrumentation, environmental noise, near surface effects, and processing procedures are exactly equal, comparison between two final migration images may show the effect of fluid movement in the reservoir. The effect may be a small difference in the travel time of an event, or any seismic change in the seismic attributes from baseline to monitor survey. Time lapse processing is a general name for the process of matching two seismic surveys in a manner that the differences between final seismic sections be only due to the changes in the reservoir's fluid boundaries or physical properties.

Probably, the first successful time lapse survey has been performed in 1987 in Holt Fireflood to show the movement of gas/oil contact (Greaves and Fulp, 1987). More than 100 time lapse seismic surveys were performed around the world by 2001 (Lumley, 2001). Time lapse studies are not restricted to the comparison of poststack images. For example, Vedanti and Sen (2009) performed prestack time lapse study by inversion of prestack data for elastic parameters to track the thermal front of an in situ combustion project.

Time lapse methods become more demanding when hydrocarbon reservoirs become old and go into the phase of tertiary recovery. Tertiary recovery phase may consist gas or solvent injection into reservoirs. Solvent injection may greatly changes the physical properties of the rocks. Physical changes must be significant enough to be tractable from their seismic responses. In addition to proper data acquisition and processing, a time lapse study is feasible in usually shallow reservoirs with unconsolidated, high porosity

and permeability, and low net pressure rocks. Otherwise, there may not be a good chance of detecting the fluid movement in the seismic sections.

Re-gridding, phase and time shift correction, and match filtering (to match the static time shift, phase, and frequency content of two surveys) are usual processing steps toward a relaible 4D seismic study. We are looking for two seismic sections from same area where any difference between time delays, amplitudes, impedance or any other attribute reflects only the changes in the physical properties in the reservoirs.

In this study, using synthetic examples, we show how different acquisition geometries between baseline and monitor surveys lead into the different migration artifacts for the same model and results in unreal time lapse effects. Loosing receivers in planted geophone surveys will leave some artifacts in the migration of monitor surveys that are different from baseline survey artifacts. We show how LSPSM can attenuate these effects and provide comparable images.

SEPARATE LSPSM INVERSION OF TIME LAPSE DATA

Through this section LSPSM is performed on the baseline and monitor surveys, separately. Joint inversion of time lapse seismic data is discussed at the next section. We show how LSPSM of time lapse datasets can help to remove the effect of different acquisition geometries or loosing receivers and provides reliable high resolution images in the next two subsections.

Reducing the effect of different acquisition geometries

Ignoring the effect of different environmental noise, near surface effects, and processing procedures, a key point to compare two pre- or poststack data from two surveys is that both, baseline and monitor surveys, have identical or similar acquisition geometries. However, this is not always feasible. The baseline survey may be an old survey with limited number of source, receivers, offsets, and foldage. Monitor surveys may use modern equipments which allow better and denser data acquisition planning and gathering. There may be some new industrial obstacles that prevent new data acquisition from matching the baseline survey pattern. For newer reservoirs, changes in acquisition geometries may be reduced by placing permanent receivers under subsurface to monitor the reservoir changes more often. However, some receivers may not function properly after a period of time. Loosing geophones will leave new artifacts in the migration image of monitor data.

In the marine data acquisition using streamers, there is a poor control on the positioning of the hydrophones due to streamer feathering. The effect of streamer feathering is greater in far offset receivers. Ocean Bottom Cable (OBC) method of data acquisition can be used instead of streamer. However, it is more expensive and have same problem as the permanently planted geophones.

Migration is always accompanied with acquisition footprints. The pattern of acquisition footprints depends on the acquisition geometry. Different acquisition geometries of old and new surveys leave different artifacts in the migrated images of the

baseline and monitor surveys. Therefore, time lapse image will show migration artifacts instead of changes in the model parameters.

Consider the baseline survey experiment as

$$\boldsymbol{d_0} = \boldsymbol{G_0}\, \boldsymbol{m_0}, \tag{1}$$

where $\boldsymbol{d_0}$, $\boldsymbol{G_0}$ and $\boldsymbol{m_0}$ are recorded data, forward modeling operator, and reflectivity for the baseline survey, respectively.

Assume the earth's reflectivity changes from $\boldsymbol{m_0}$ to $\boldsymbol{m_1}$ after a period of time as:

$$\boldsymbol{m_1} = \boldsymbol{m_0} + \boldsymbol{\Delta m}, \tag{2}$$

where $\boldsymbol{m_1}$ is the reflectivity at the time of monitor surveying, and $\boldsymbol{\Delta m}$ is the difference in reflectivity between two data acquisition. Monitor surveying records data, $\boldsymbol{d_1}$, which mathematically is expressed by

$$\boldsymbol{d_1} = \boldsymbol{G_1}\, \boldsymbol{m_1}, \tag{3}$$

where $\boldsymbol{G_1}$ is the forward modeling operator of the monitor survey.

Migration of two surveys gives:

$$\widehat{\boldsymbol{m_0}} = \boldsymbol{G_0^T}\, \boldsymbol{d_0}, \tag{4}$$

for the baseline survey and

$$\widehat{\boldsymbol{m_1}} = \boldsymbol{G_1^T}\, \boldsymbol{d_1}, \tag{5}$$

for the monitor survey, where $\widehat{\boldsymbol{m_0}}$ and $\widehat{\boldsymbol{m_1}}$ are migration of baseline and monitor surveys, respectively.

Even when model is not changing, $\boldsymbol{m_1} = \boldsymbol{m_0}$, $\widehat{\boldsymbol{m_0}}$ and $\widehat{\boldsymbol{m_1}}$ will be different due to different acquisition parameters between $\boldsymbol{G_0}$ and $\boldsymbol{G_1}$.

When two acquisition geometries are similar and change in the velocity of the modeling operators is negligible, $\boldsymbol{G_0} \sim \boldsymbol{G_1}$, we may write:

$$\widehat{\boldsymbol{m_1}} = \boldsymbol{G_0^T}\, \boldsymbol{d_1} = \boldsymbol{G_0^T}\, \boldsymbol{G_0}\, \boldsymbol{m_1} = \boldsymbol{G_0^T G_0}\, (\boldsymbol{m_0} + \boldsymbol{\Delta m}) = \widehat{\boldsymbol{m_0}} + \boldsymbol{G_0^T G_0}\, \boldsymbol{\Delta m}, \tag{6}$$

or,

$$\widehat{\boldsymbol{m_1}} - \widehat{\boldsymbol{m_0}} = \boldsymbol{G_0^T G_0}\, \boldsymbol{\Delta m}, \tag{7}$$

which states that the difference between baseline and monitor migration images is proportional to the changes in the model parameters between two survey. However, since $\boldsymbol{G_0^T G_0}$ is not a unitary operator, the difference in migration images is not exactly equal to the real changes in the reflectivity.

Migration images, $\widehat{\boldsymbol{m_0}}$ and $\widehat{\boldsymbol{m_1}}$, must be cross-equalized to remove the effect of non-repeatability of data acquisition and migration artifacts before generating the time

lapse image. Few cross-equalization methods have been proposed. For example, Rickett and Lumley (2001) suggested a cross-equalization flow including two run of match filter application after re-gridding data for amplitude, phase and bandwidth balancing.

LSPSM is an effective method to reduce the acquisition artifacts to make the final images comparable (Nemeth, et al., 1999). Separate damped LSPSM of the baseline survey

$$\boldsymbol{m_{DSL0}} = \left(\boldsymbol{G_0^T}\,\boldsymbol{G_0} + \mu_0^2\boldsymbol{I_0}\right)^{-1}\boldsymbol{G_0^T}\,\boldsymbol{d_0}, \tag{8}$$

and monitor survey

$$\boldsymbol{m_{DSL1}} = \left(\boldsymbol{G_1^T}\,\boldsymbol{G_1} + \mu_1^2\boldsymbol{I_1}\right)^{-1}\boldsymbol{G_1^T}\,\boldsymbol{d_1}, \tag{9}$$

provides images that are less affected by the corresponding acquisition geometries. Therefore, they represent the changes in the reflectivity model better than the migration images. It means when $\boldsymbol{m_1} = \boldsymbol{m_0}$,

$$\boldsymbol{m_{DSL0}} \sim \boldsymbol{m_{DSL1}}, \tag{10}$$

even when $\boldsymbol{G_0} \neq \boldsymbol{G_1}$.

In addition to this, the ability of data reconstruction by LSPSM provides another reliable domain for comparison between two surveys, data domain. Datasets reconstructed from two surveys into a new geometry make the prestack time lapse studies more feasible and reliable.

In this subsection, using a synthetic dataset, we compare the differences between migration and LSPSM images from same model and with different geometries for the baseline and monitor surveys. We follow the methodology in equations 8 and 9 to compute the LSPSM images of the baseline and monitor surveys. The joint inversion of two datasets is explained in next section of this paper.

I also show the reconstructed data from two surveys and compare them with the original data. For these purposes, consider the velocity model in Figure 1. We compare the data generated using this model with two different geometries as the baseline and monitor surveys without any change in the model parameters through this and next subsections.

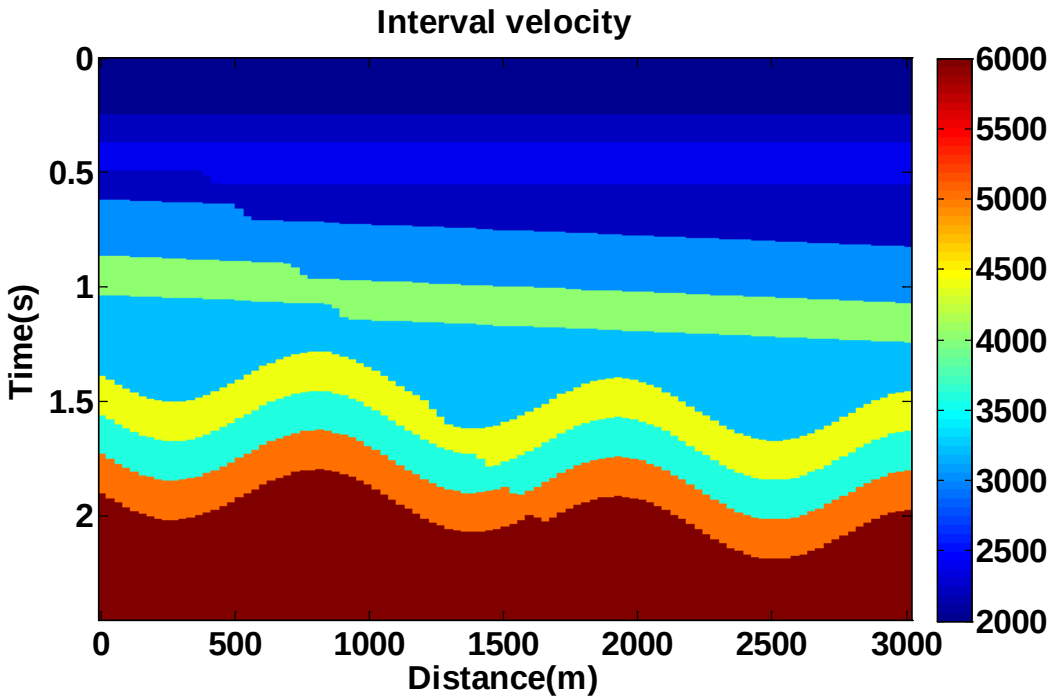

FIG. 1. Velocity model used for forward modeling and data generation.

Case I: both surveys have dense data sampling

Suppose the baseline survey has the acquisition geometry shown in Figure 2a. There are 32 sources and 100 receivers per source. Source spacing is about 100m and receiver spacing chosen to be 18m to have foldage at 10. Acquisition geometry of the monitor survey, shown in Figure 2b, includes 20 sources and 200 receivers per source. The source spacing is 150m and receiver spacing chosen at 15m to keep foldage at 10. Baseline and monitor synthetic data are generated with these geometries and 1% random noise is added to both datasets. Source wavelet and the other parameters are equivalent for both experiments. These geometries are significantly different. However, due to dense sampling, they should produce accurate migration images. Consequently the difference between two migration images should be negligible.

In the following subsections, we show that this is not necessarily true. Even a dense data sampling produces a type of acquisition footprints which may be different from the acquisition footprints of the second dense survey of the same area. It is then shown how LSPSM can improve the time lapse imaging.

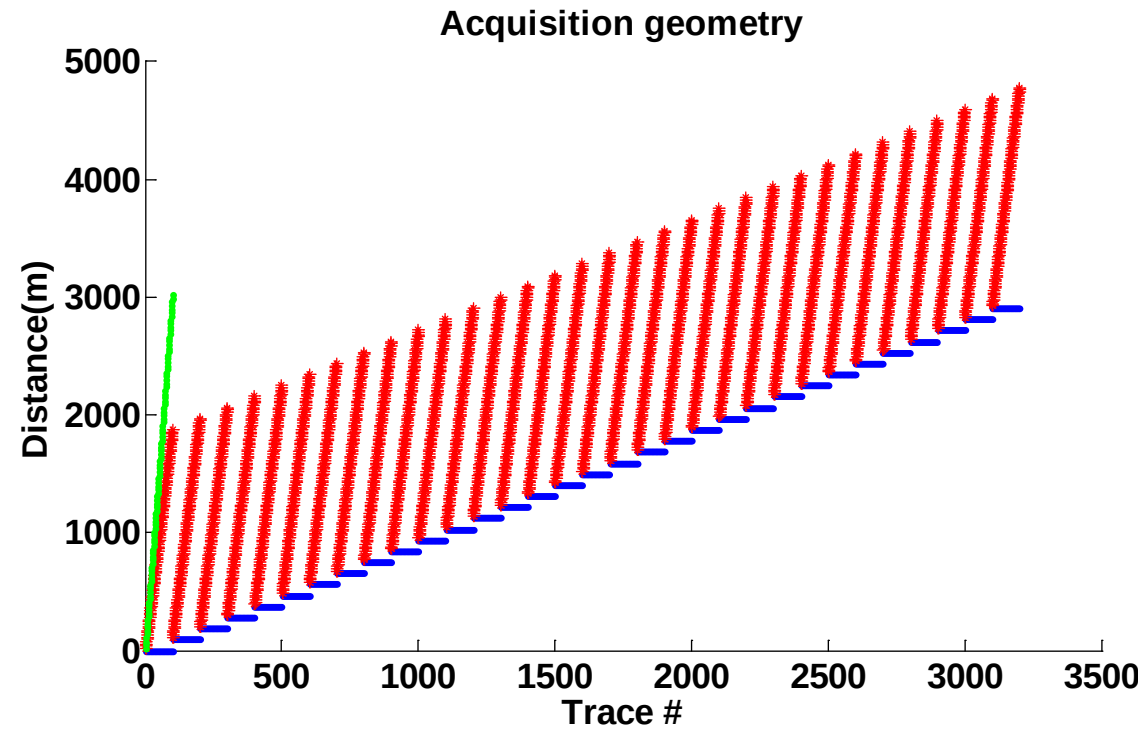

a)

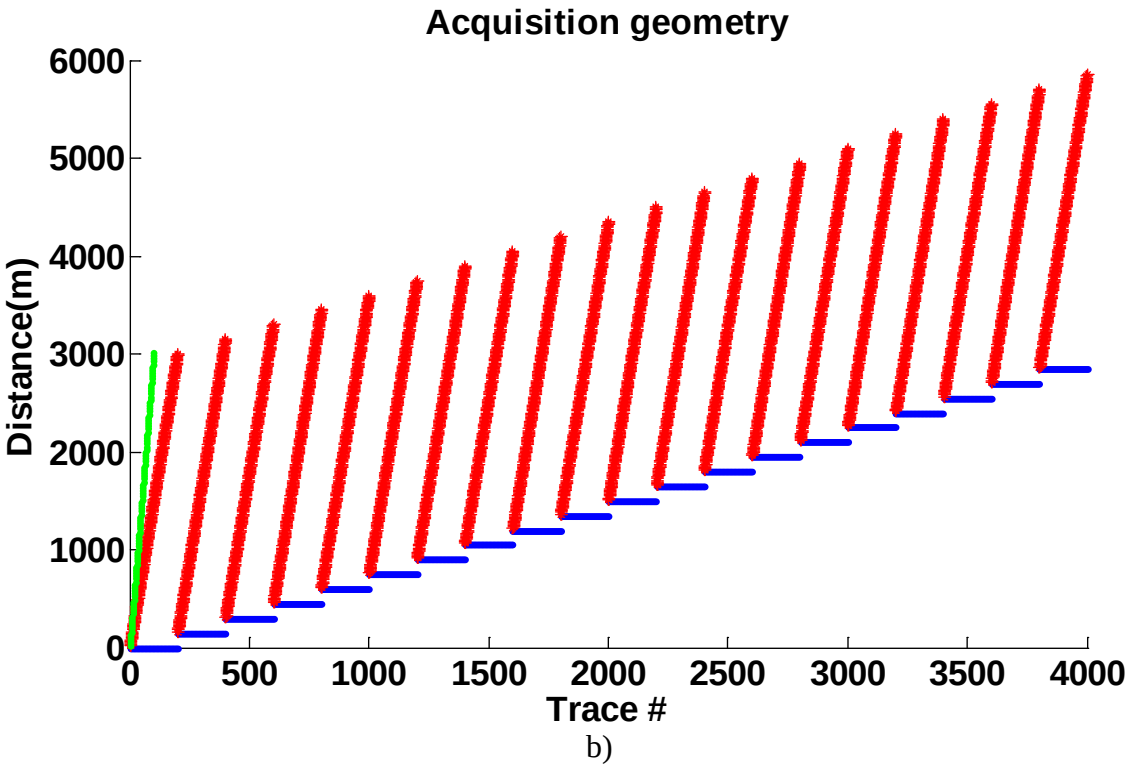

b)

FIG. 2. Acquisition geometry for baseline (a) and monitor (b) surveys. Blue: sources, red: receivers, green: image points.

Comparing migration and LSPSM images for poststack time lapse studies:

Migration images resulted from baseline and monitor surveys are shown in Figure 3. All migration parameters are identical for both surveys. Exact velocity model is used in migration. Both images have good quality. To perform a comparison between these two migration, monitor image is subtracted from baseline image. The difference image is shown in Figure 4. Since the velocity model is not changing between these two surveys, the difference should be zero or an image showing the difference between random noise of the two survey. However, due to the presence of different acquisition footprints, the difference image shows some changes in the model which are not due to the changes in the physical properties of the model.

Figure 5 shows the LSPSM images for both, baseline and monitor surveys. Both datasets produced high resolution images. Figure 6 shows the difference between two LSPSM images. Comparing Figure 4 with Figure 6 show that the LSPSM method has significantly reduced the acquisition footprints and returned images which are more reliable than the migration images for a time lapse study. It is very important in any poststack time lapse study that both surveys be less affected from surveying effects, as much as possible.

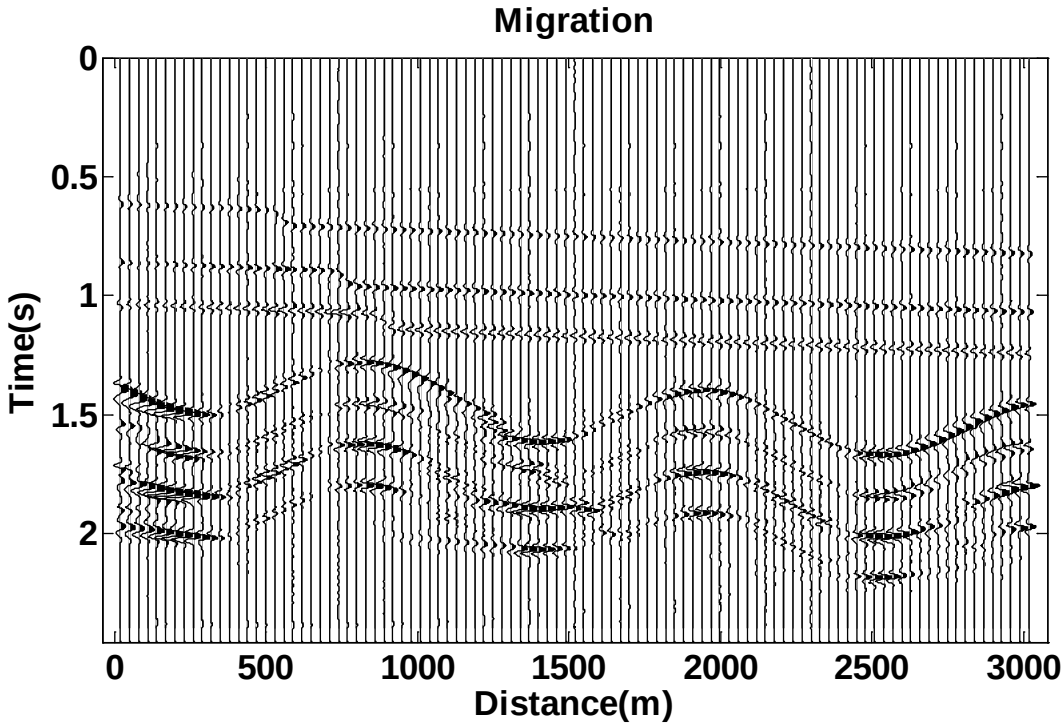

a)

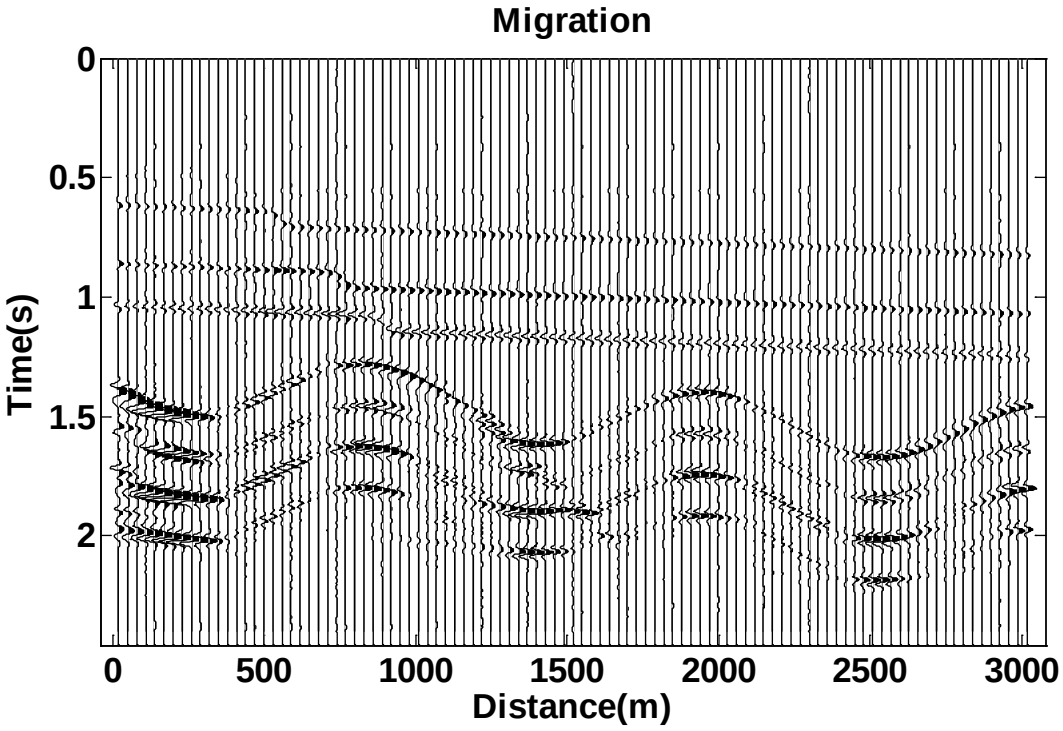

b)

FIG. 3. Migration of dataset from baseline (a) and monitor (b) survey.

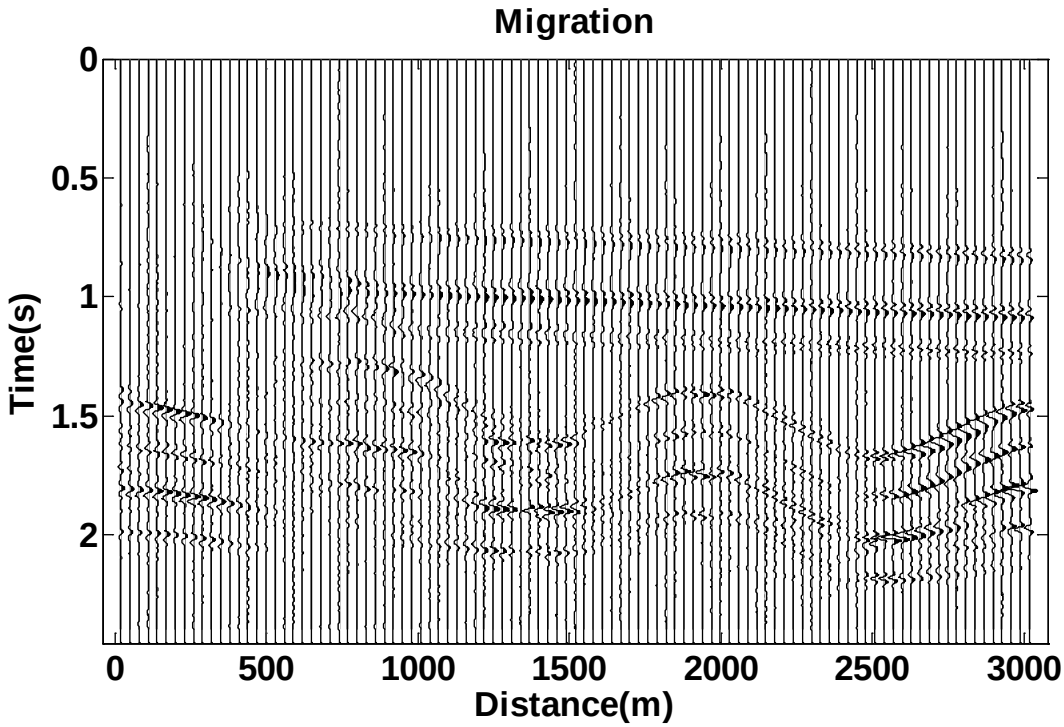

FIG. 4. The difference between two migration images in Figure 3.

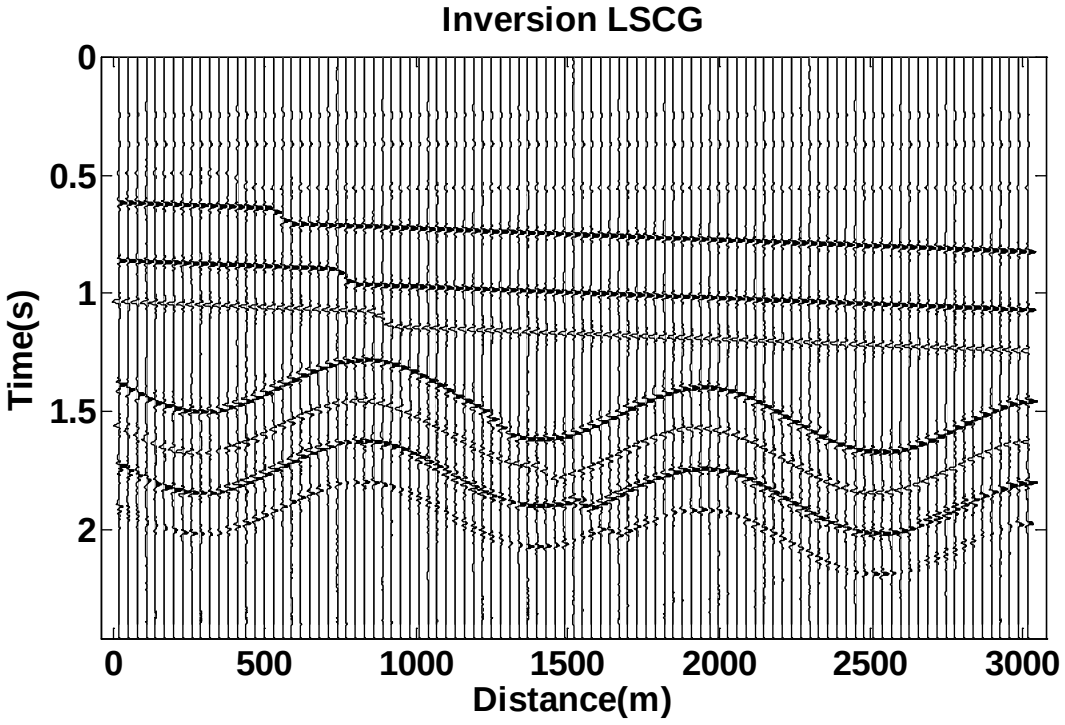

a)

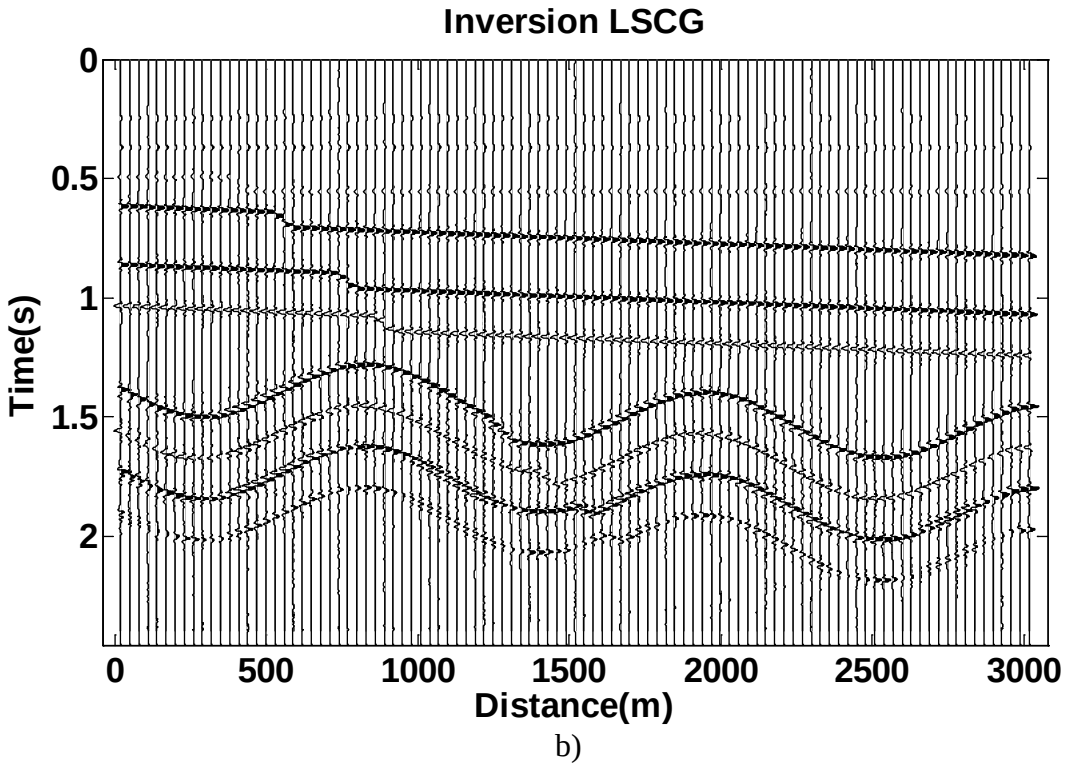

b)

FIG. 5. LSPSM images of the dataset from baseline (a) and monitor (b) surveys.

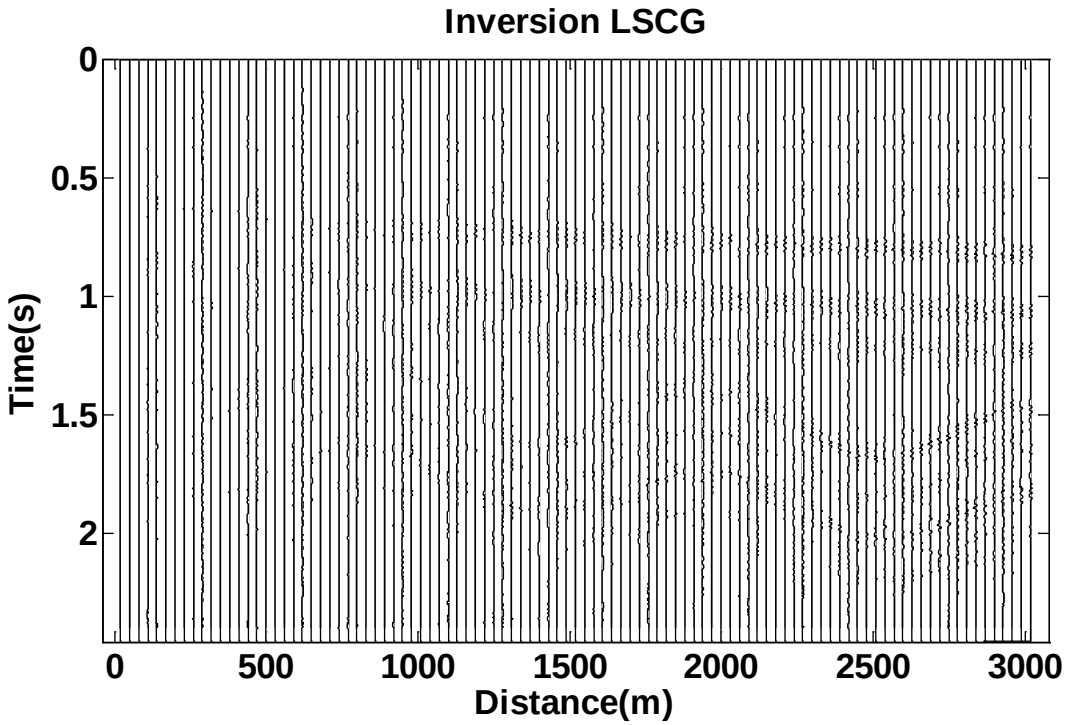

FIG. 6. The difference between two LSPSM images in Figure 5.

Comparing data and reconstructed data for prestack time lapse studies:

Prestack time lapse studies provide very useful information about fluid flow using AVO methods. Noise and other undesired events such as multiples may get attenuated by stacking or migration, but they remain in the prestack data. In addition, prestack data are more affected by the different acquisition geometries of the baseline and monitor surveys. Therefore, prestack time lapse studies require more attention to detail when considering time lapse differences. Two surveys may have different offset spacing for the same CMP gather. Data reconstruction by LSPSM provides two new baseline and monitor datasets for a given geometry in which CMPs have equivalent number of traces and offsets. A given geometry can be either baseline or monitor acquisition geometry or a new desired designed survey. Consequently, data reconstructed for two surveys are made comparable.

For instance, consider a CMP point at 2000m in previous example. Figure 7 show the CMP gather from baseline (a) and monitor (b) surveys. Both CMP gathers have 10 traces. However, the comparison is not feasible because of the differences in the traces' offsets. Subtracting the two CMP gathers results the CMP in panel (c) in Figure 7, which is not a logical subtraction.

Using LSPSM method and with the geometry of baseline survey, data from both surveys are reconstructed. Figure 8 shows the reconstructed data from baseline survey, monitor survey and the difference for a CMP at 2000m position. Since there is not any change in the model parameters, two reconstructed CMP gathers are similar and the difference panel shows very low energy residuals. Therefore, data reconstruction of both, baseline and monitor surveys, makes the prestack time lapse study feasible. This is very useful in the AVO inversion studies before and after fluid or steam injection to track the

movements of fluid/gas boundary or changes in the reservoir temperature due steam injection.

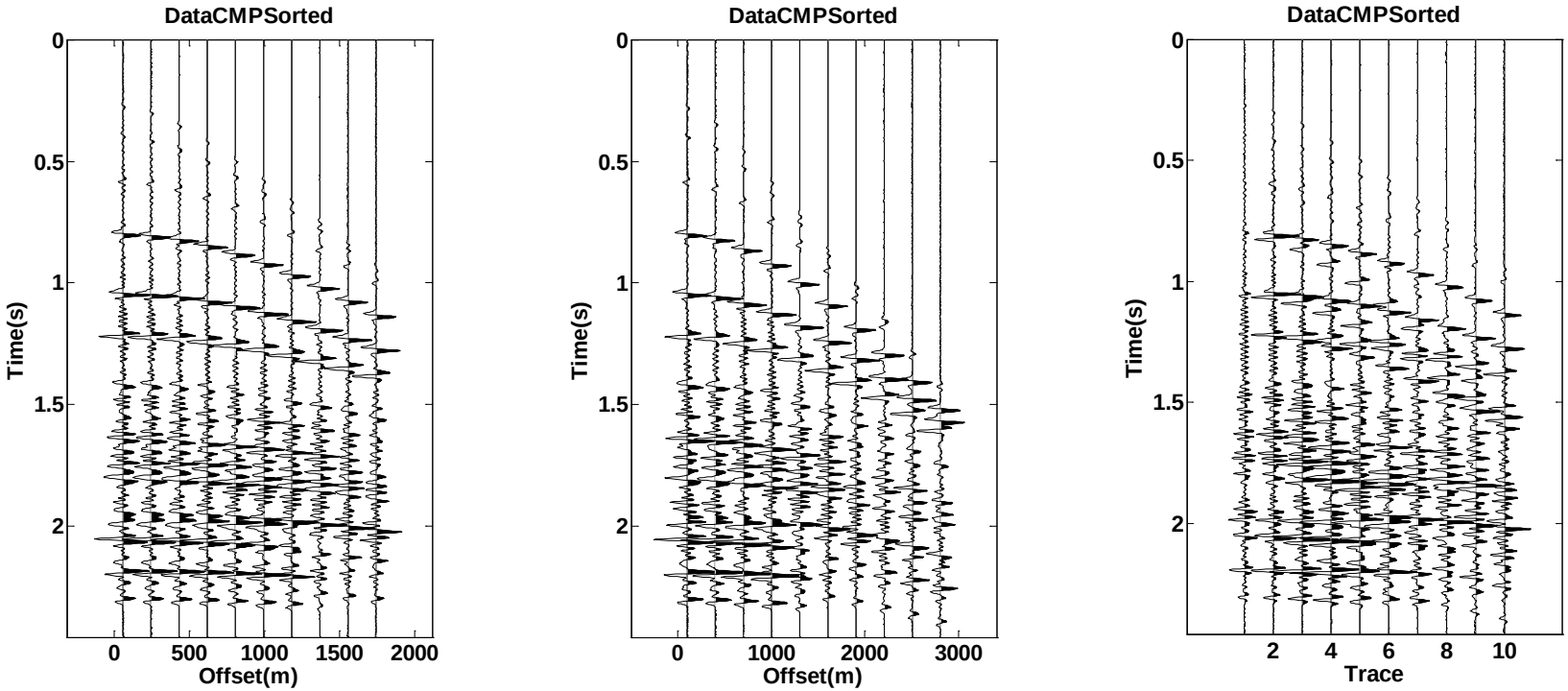

a) b) c)

FIG. 7. CMP gathers from baseline (a) and monitor (b) surveys and their difference (c).

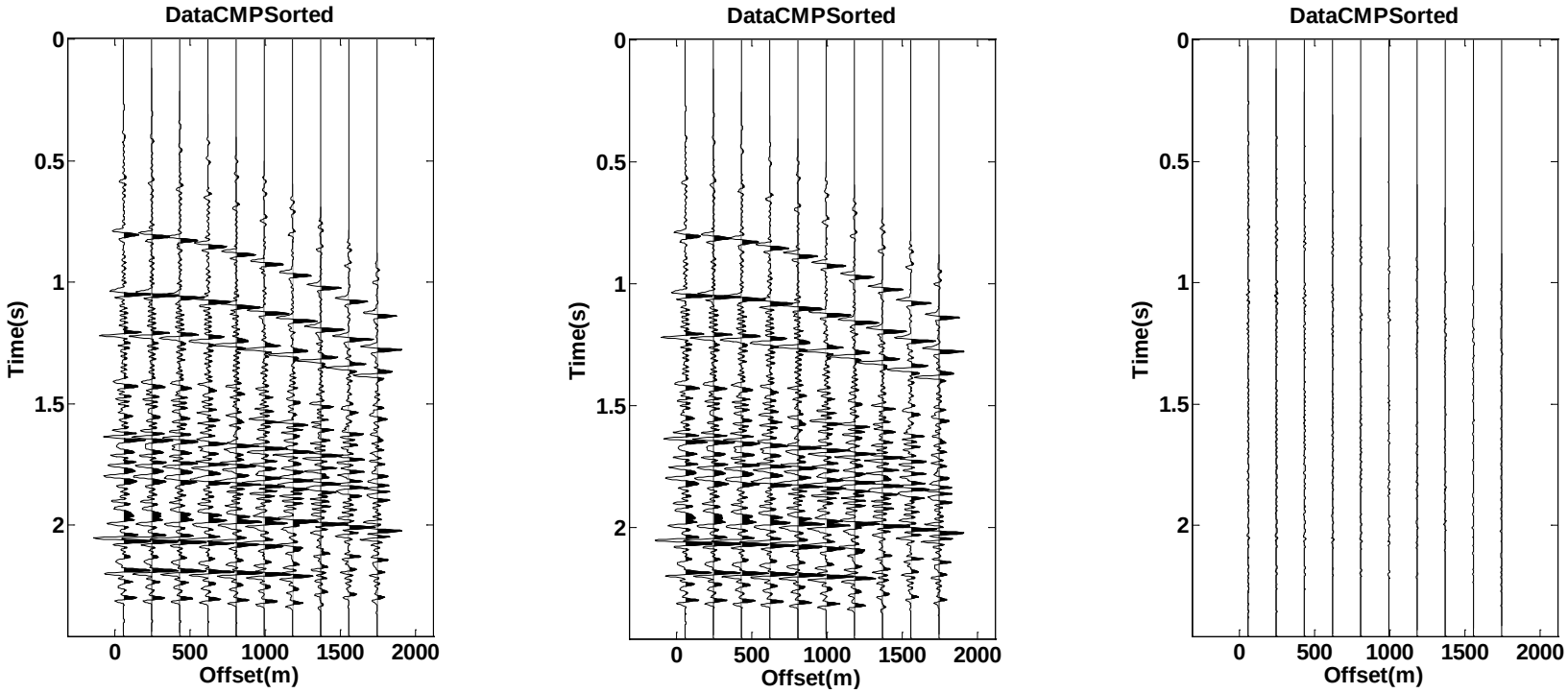

a) b) c)

FIG. 8. Reconstructed CMP gathers from baseline (a) and monitor (b) surveys and difference (c).

Case II: both surveys are 80% decimated

In the example at the previous section both surveys had very dense and regular data sampling. With a coarse and irregular data sampling, migration images will have more acquisition artifacts and time lapse studies become unreliable. Prestack data of the two surveys will also have very irregular offset spacing in the CMP gathers. In such cases implementation of an imaging method which is less affected from irregular sampling is very important. We show the ability of LSPSM for making time lapse study of very irregular sampled data possible.

Consider the same baseline and monitor surveys as in the previous section. We randomly removed 80% of data from both surveys. Figure 9 show the resulted acquisition geometries. Decimated data from the two surveys are migrated. Figure 10a shows the difference between two migration images. Acquisition footprints left many artifacts in this image which makes the poststack time lapse study be unreliable. However, most of these artifacts are removed by LSPSM method as seen in Figure 10b which shows the difference between LSPSM images from baseline and monitor survey datasets.

Prestack time lapse study for this experiment is almost impossible due to the limitation of traces in each CMP gather. An industrial solution is merging adjacent CMP gathers to a supergather. Figure 11 show two CMP supergathers for the baseline and monitor surveys. Five adjacent CMP are combined to create these gathers. Due to irregularities in the offset position of traces, the comparison between two gathers is not practical. Figure 12 shows the reconstructed data which are CMP sorted. LSPSM is used for data reconstruction of decimated data from both surveys into the undecimated baseline survey. Residual in panel (c), the difference between two reconstructed CMPs, has very low energy signals.

Therefore, any subtle changes in the physical properties of the reservoir rocks which are detectable by seismic method, would be tractable in the LSPSM reconstructed data.

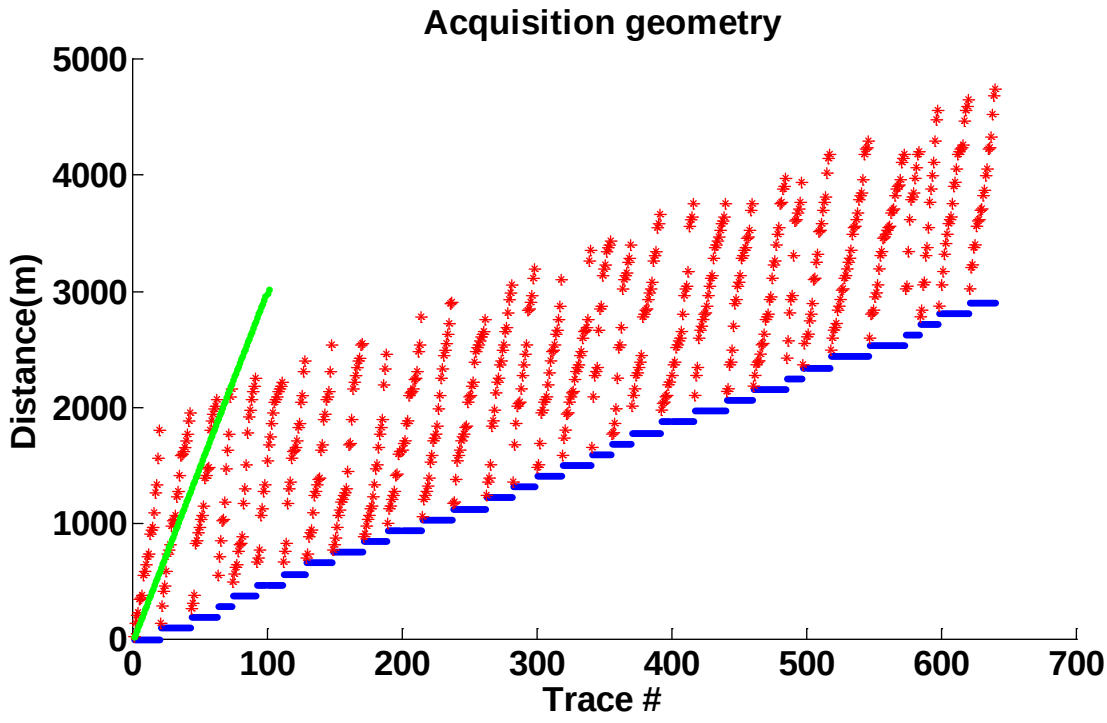

a)

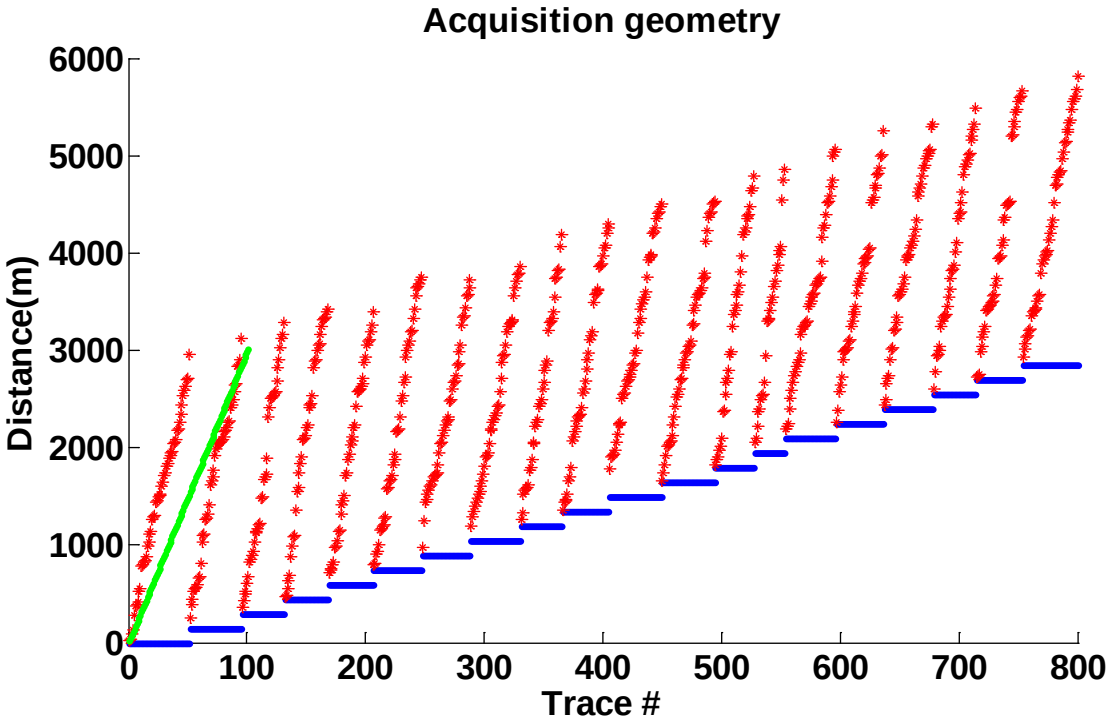

b)

FIG. 9. Acquisition geometry for decimated baseline (a) and monitor (b) surveys. Blue: sources, red: receivers, green: image points.

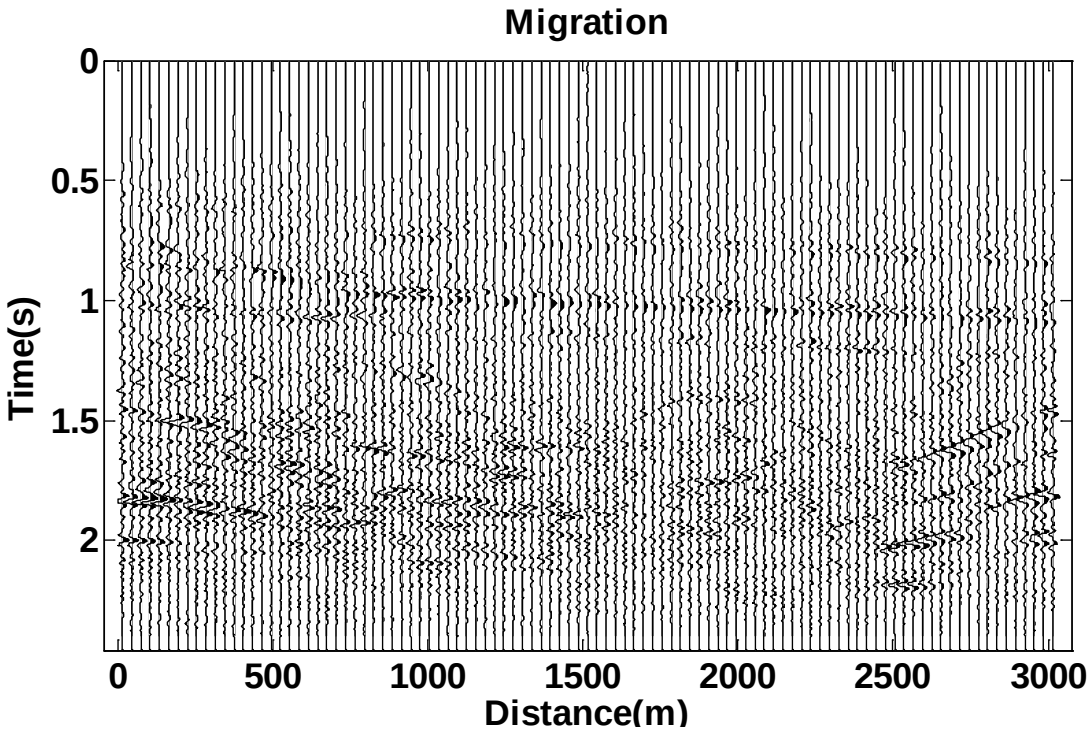

a)

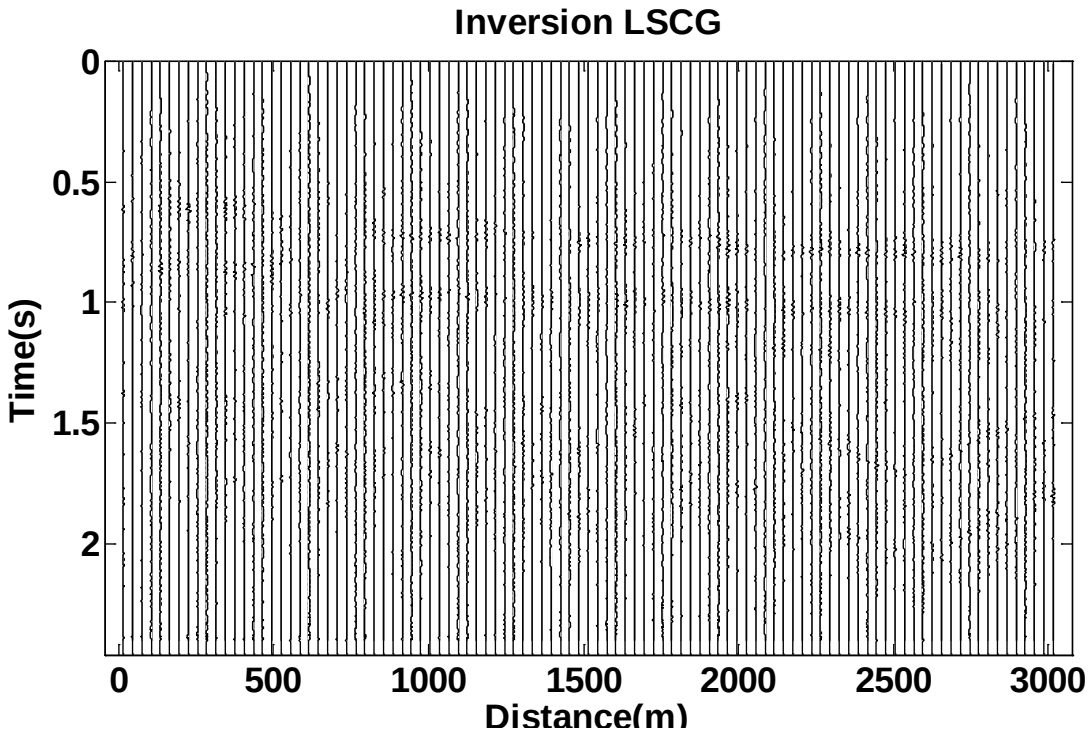

b)

FIG. 10. The difference between two migration (a) and LSPSM (b) images.

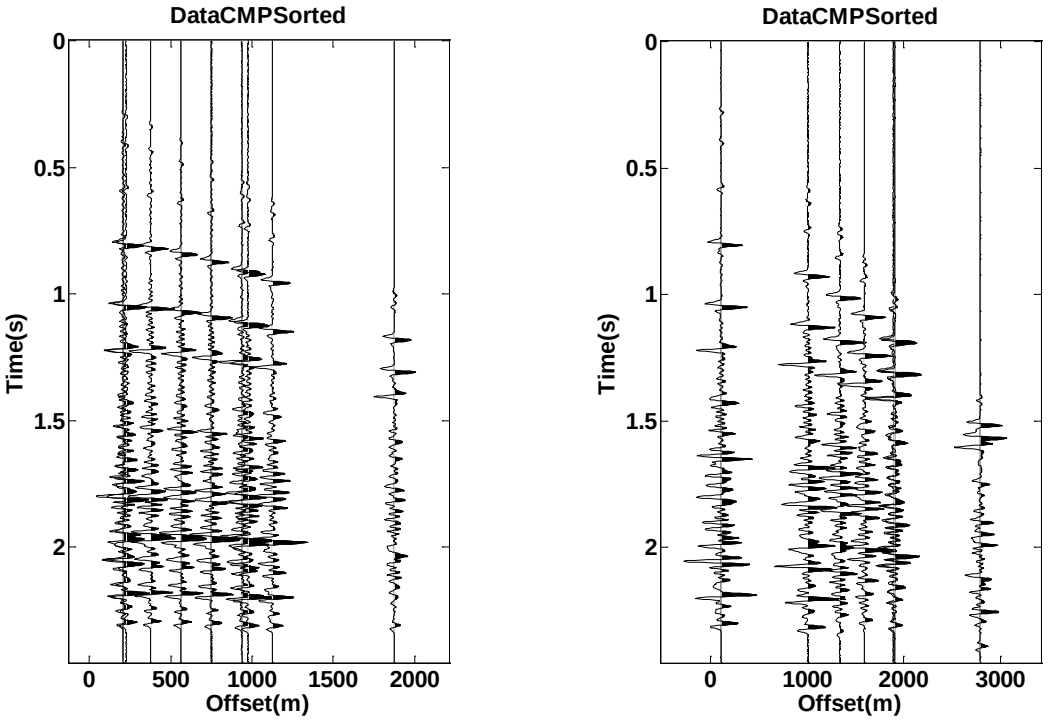

a) b)

FIG. 11. CMP-bin supergathers from baseline (a) and monitor (b) surveys.

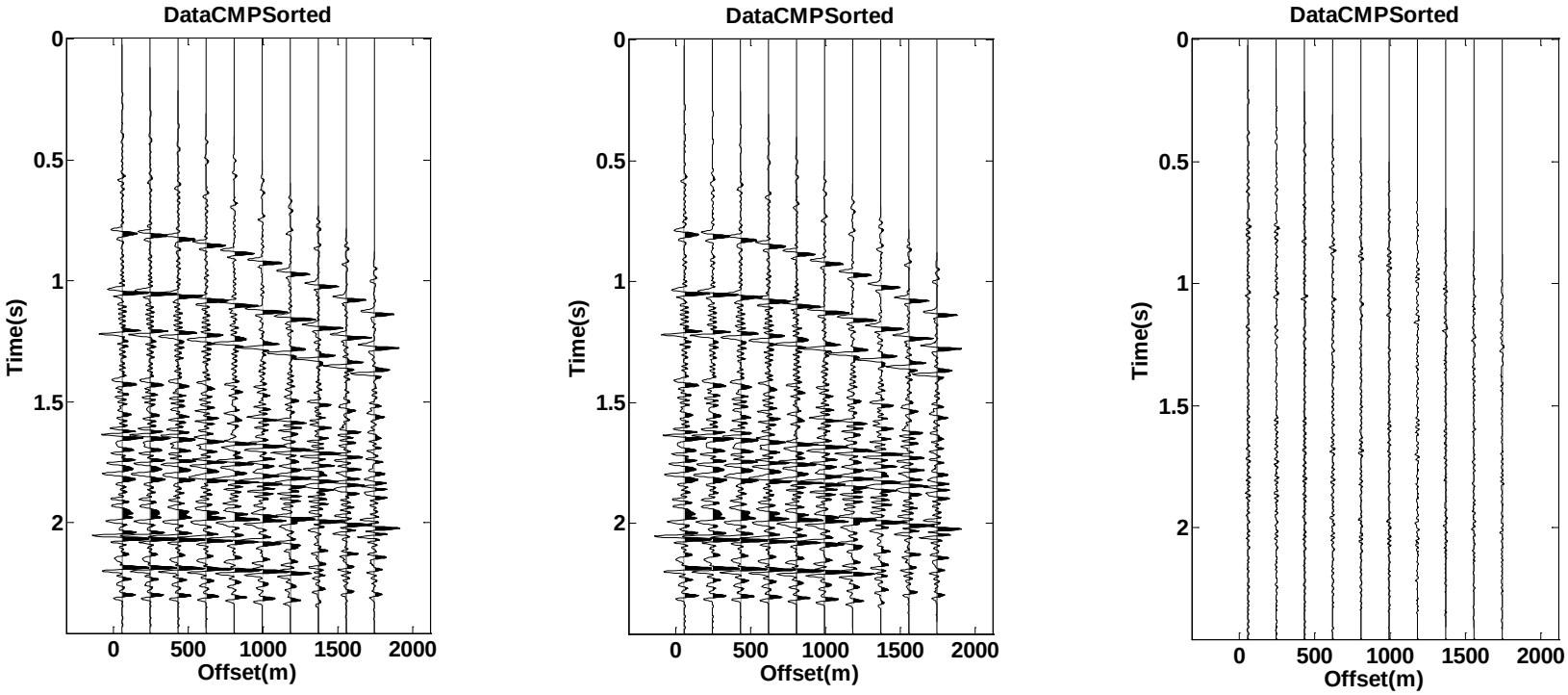

a) b) c)

FIG. 12. Reconstructed CMP gathers from baseline (a) and monitor (b) surveys and their difference (c).

Reducing the effect of loosing receivers

The ability of the LSPSM for reducing the effects of different acquisition geometries in the baseline and monitor surveys is shown in the previous sections. Attempt to mimic baseline acquisition geometry in the monitor surveys may be replaced by permanently planting receivers on the ground or at a very shallow depth. In marine, streamer acquisition may be replaced by OBC and cable left at the bottom of sea for the future monitor data acquisitions. Replacing streamer with the OBC method is more beneficial since it makes the shear waves recording possible too. In both methods, planted geophones or OBC, the receivers geometry remains unchanged. Consequently, similar acquisition artifact patterns will be introduced into the migration images and time lapse studies are feasible.

However, after a period of time some receivers may not function properly. Therefore, monitor surveys become affected by having less number of receivers as the deployed receiver system becomes older. Loosing receivers by time produces more artifacts in the monitor survey migration images. In order to have the same artifacts in the baseline survey, traces that correspond to the dead geophones must be removed from the baseline data. Alternatively, we show how this effect can be minimized by replacing migration with the LSPSM method. Separate LSPSM of the baseline and decimated data provides images that are less than migration image affected by the effect of loosing receivers.

Comparing migration and LSPSM images

Consider the baseline survey in the previous section. We assume that six monitor seismic surveys are performed in this area with planted receivers. Source positions are not changing from baseline to monitor survey. We are assuming a large percent of receivers are not functioning with newer monitor surveys. Baseline survey has 3200 traces. However, only 50, 30, 20, 10, 5, and 2% of traces are functioning in the future monitor surveys. Last three cases are very extreme and not realistic. Data from monitor survey migrated and LSPSM inverted. The left hand side panels of Figure 13 shows the difference between migration of baseline data and six monitor surveys while the right hand side panels show the difference between LSPSM image of baseline data and six monitor surveys. As shown, by losing more receivers, due to more acquisition footprints in the monitor surveys, the difference between migration images significantly increases. LSPSM images are less affected by loosing receives and there is no noticeable difference between baseline LSPSM image and monitor LSPSM images. Since it can produces a high resolution time lapse image, using LSPSM to compensate for the difference in acquisition artifacts is a better choice than the ignoring some receivers from baseline survey to make it similar to monitor survey.

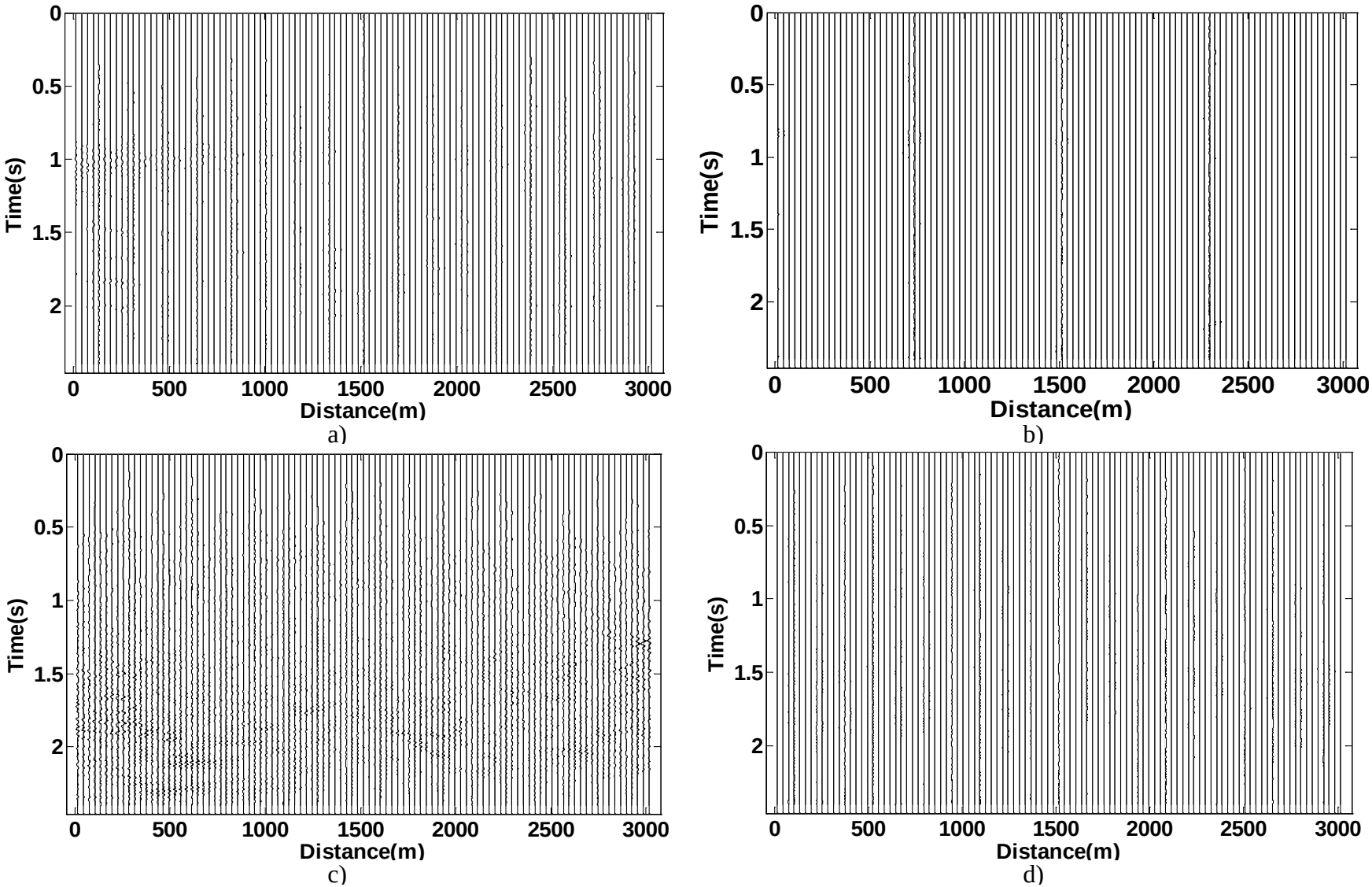

FIG. 13. Migration difference (a and c) and LSPSM difference (b and d) with using 50% (a and b) and 30% (c and d) of data.

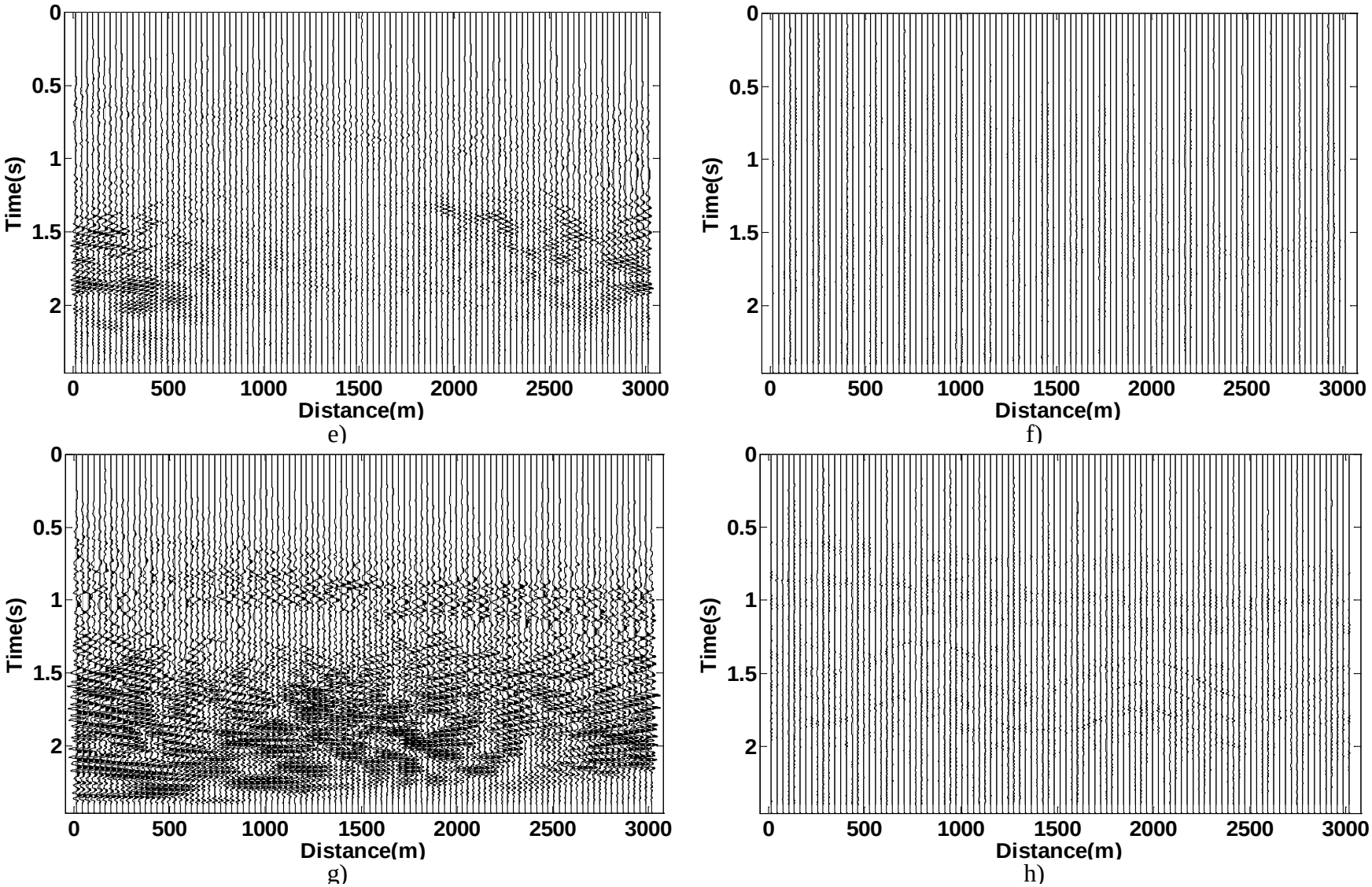

FIG. 13 Contd: using 20% (e and f) and 10% (g and h) of data.

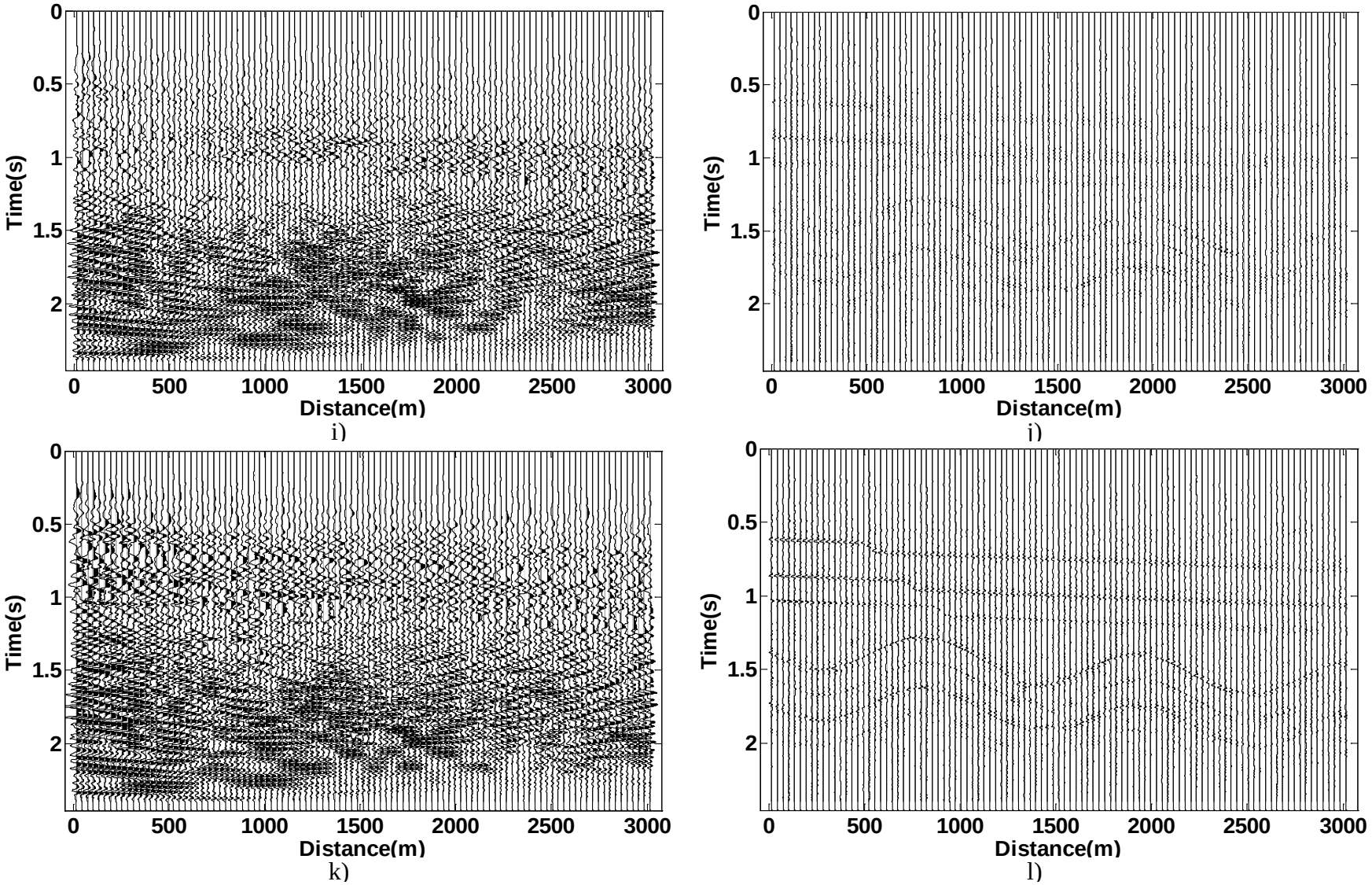

FIG. 13. Contd: using 5% (i and j) and 2% (k and l) of data.

Comparing data and reconstructed data from two surveys

Figure 14 shows the effect of loosing receivers in the monitor surveys on a CMP gather at the position of 2000m. Losing more receivers in the newer surveys make the comparison between prestack datasets more difficult. However, as Figure 15 shows, data reconstructed by LSPSM are comparable and the difference between original and reconstructed data is a very low energy CMP gather. Therefore, effect of loosing receivers can be compensated by data reconstruction with LSPSM. This method helps keeping the foldage in the same level as the baseline survey for comparing AVO effects of the baseline and monitor surveys.

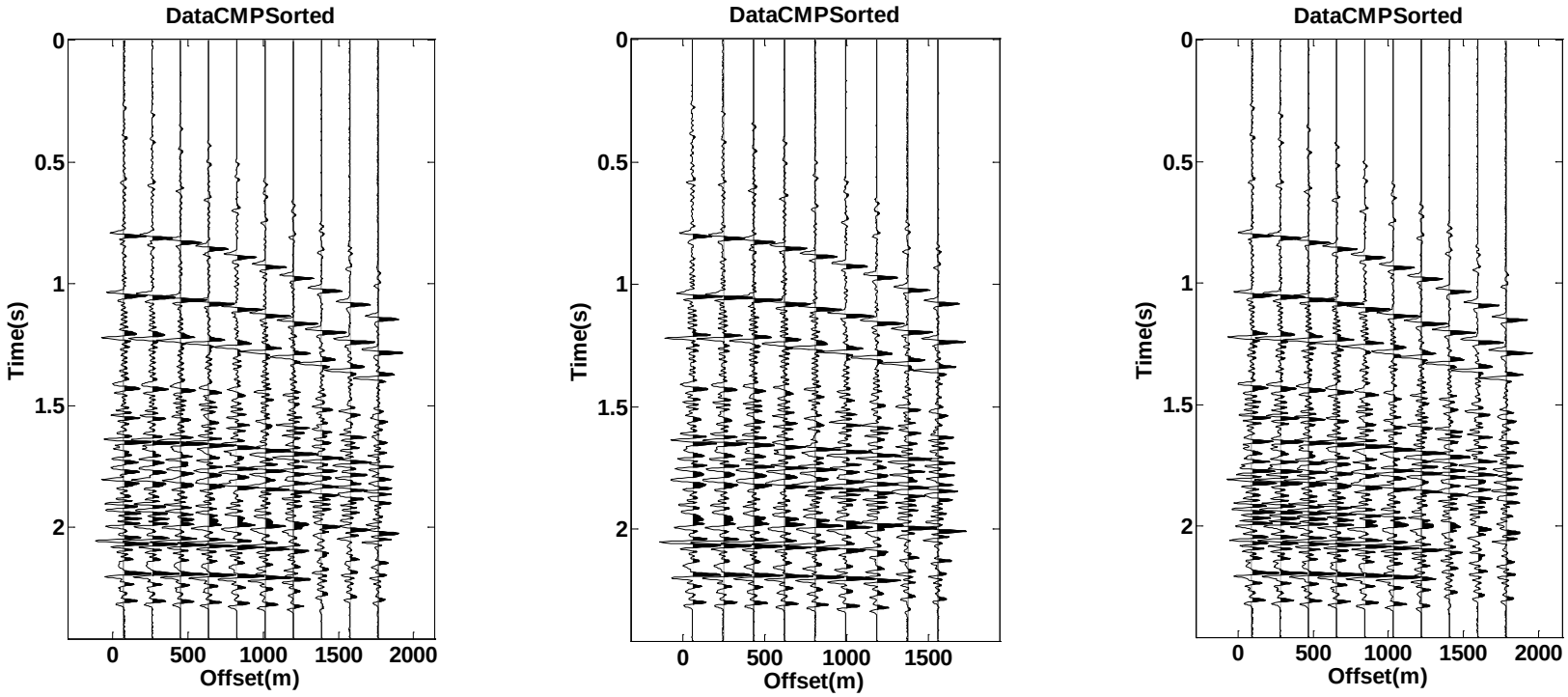

a) b) c)

FIG. 14. CMP gathers from monitor surveys after 50, 30, 20, 10, 5, and 2% in panels (a), (b), (c), (d), (e), and (f), respectively.

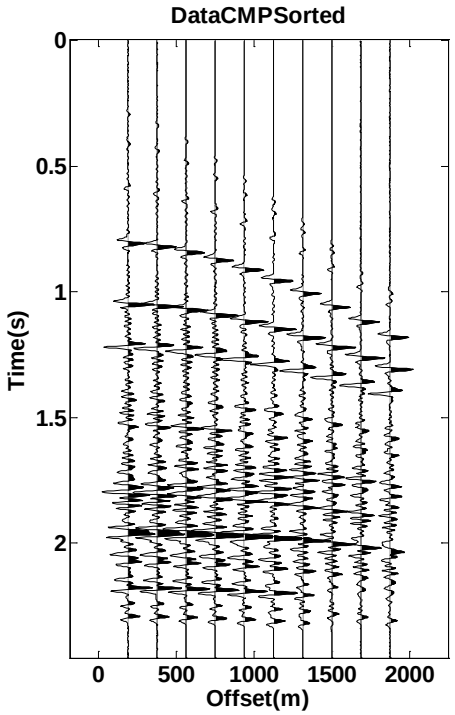

d)

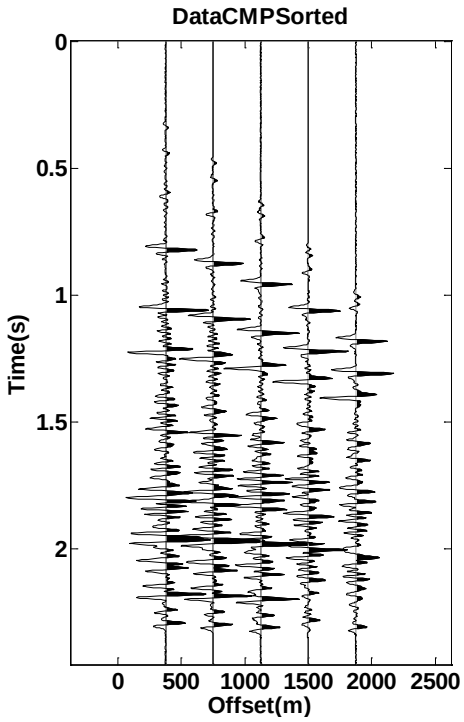

e)

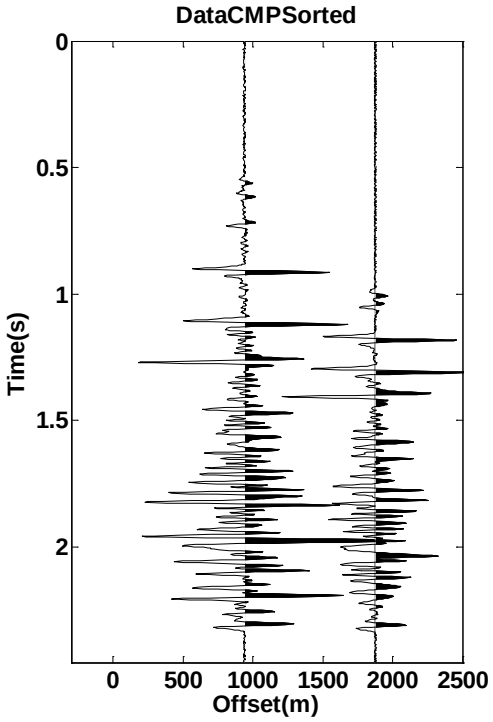

f)

FIG. 14. Contd.

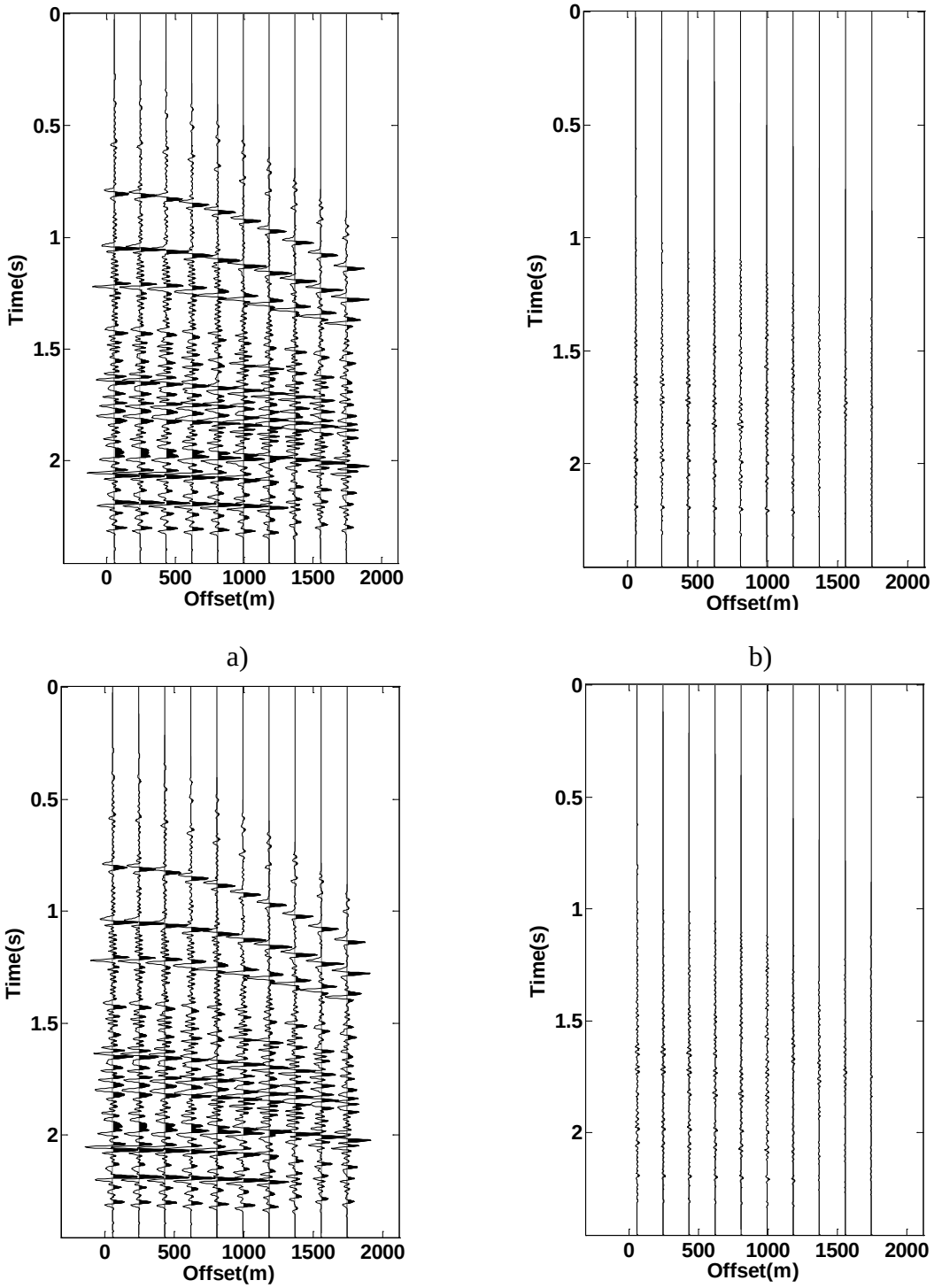

FIG. 15. Reconstructed CMP gathers using LSPSM on the left and the d. (a,c) and difference from baseline data on the right, with (a,b) 50%, (c,d) 30%, (e,f) 20%, (g,h) 10%, (i,j) 5%, and (k,l) 2% of data.

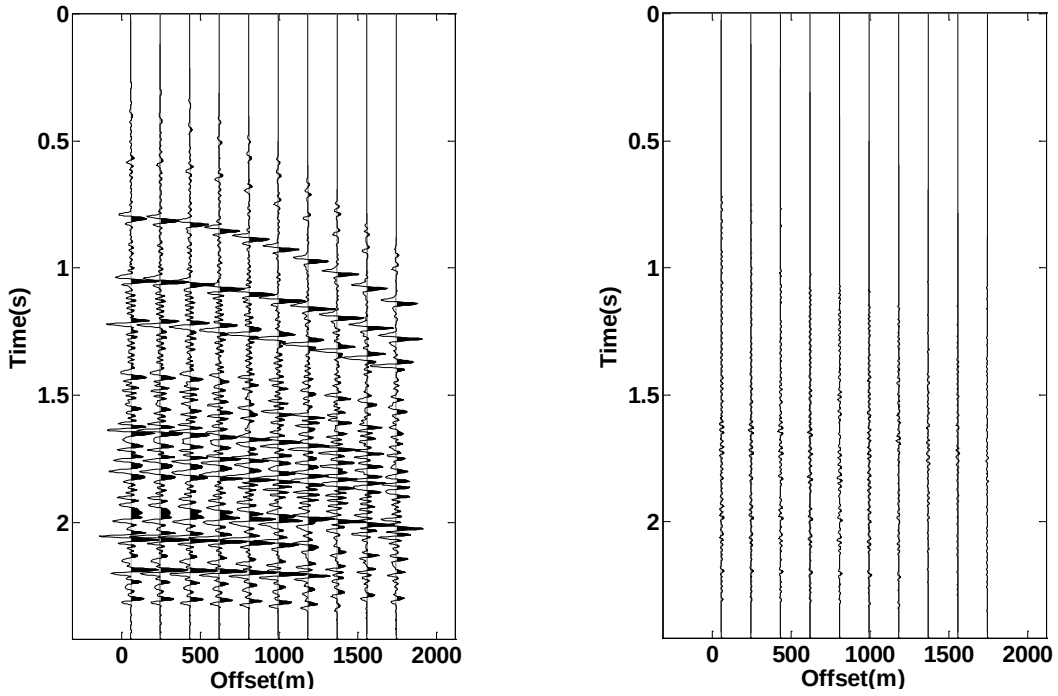

e) f)

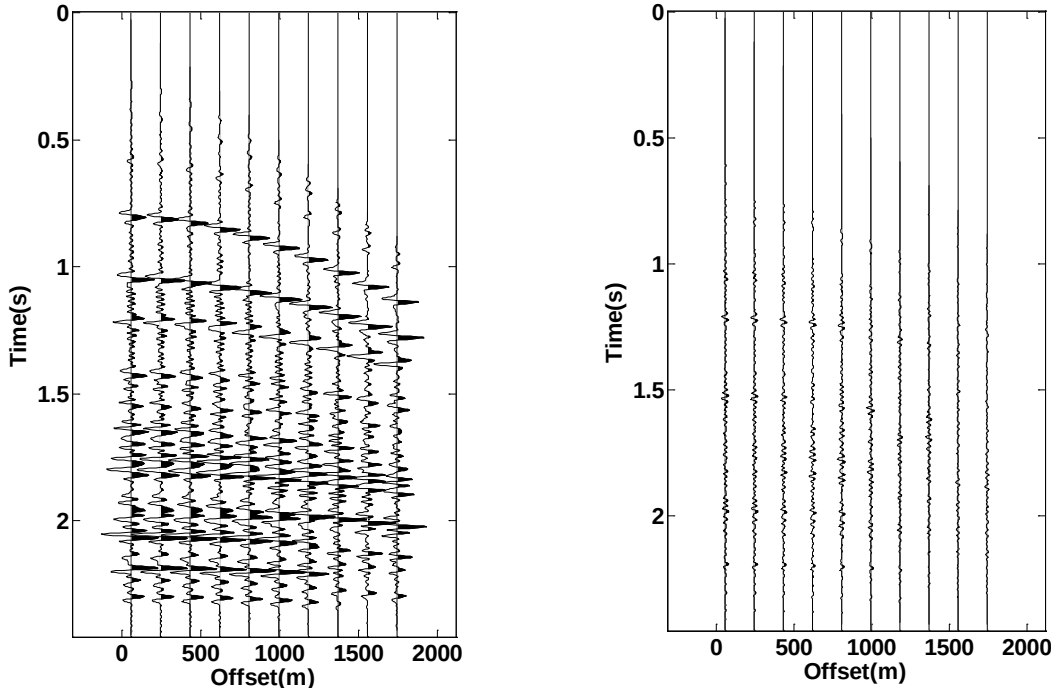

g) h)

FIG. 15. Contd.

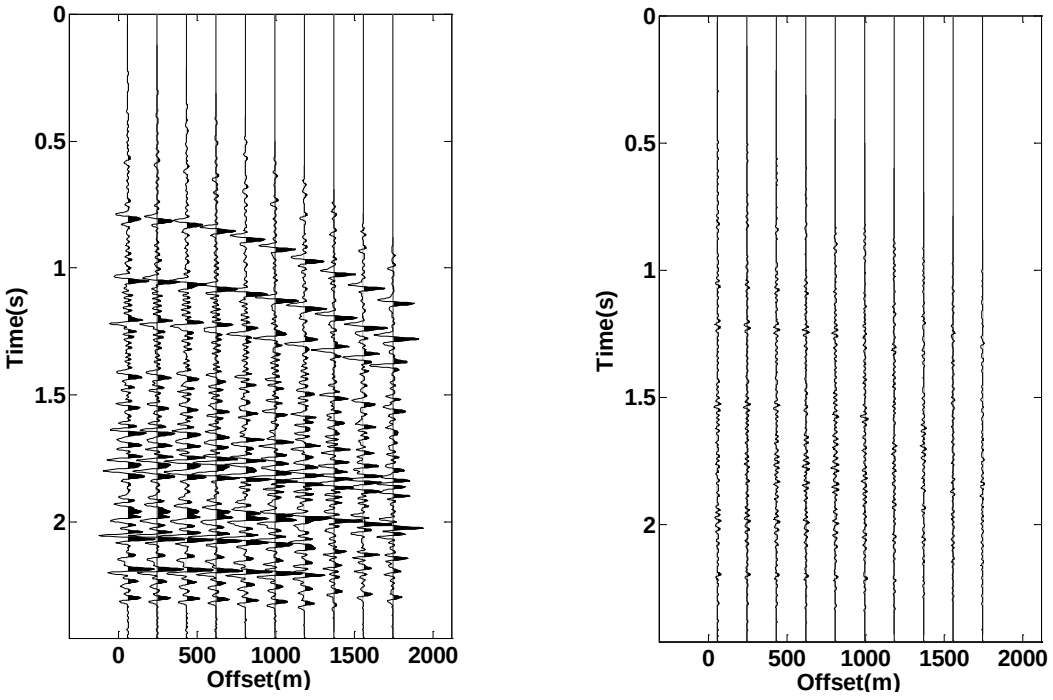

i) j)

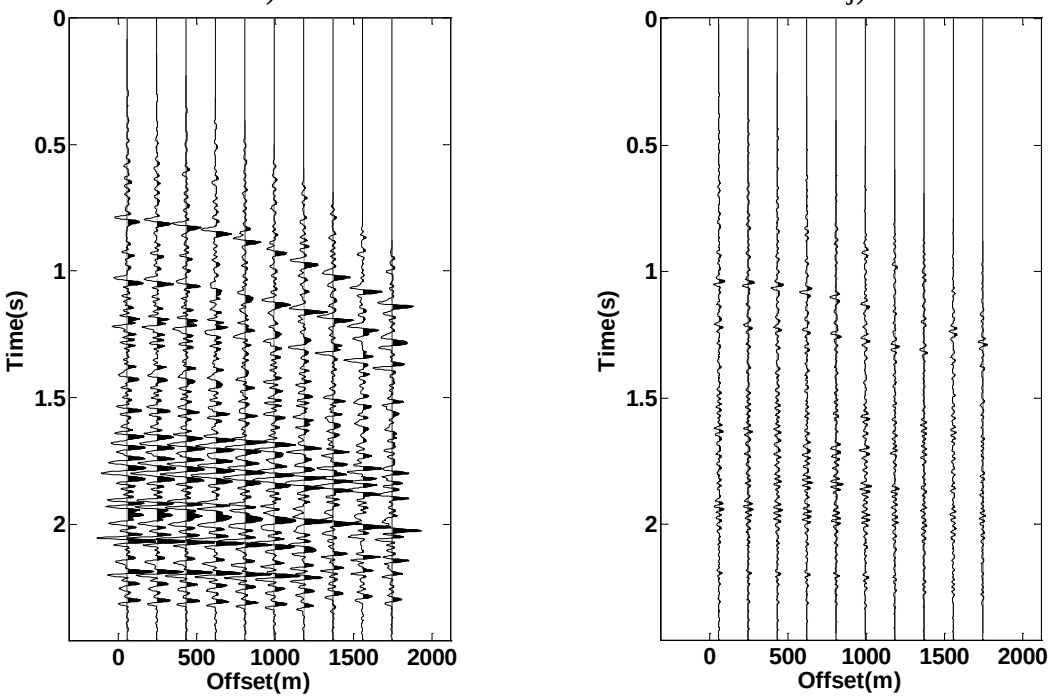

k) l)

FIG. 15. Contd.

High resolution detection of the reflectivity changes

In this section we assume that the baseline and monitor surveys have similar geometries but velocity and consequently the reflective model changes from baseline to monitor survey. We compare the baseline and monitor migration and LSPSM images change.

Consider the baseline geometry at the bingeing of this report as the baseline and monitor surveys geometries. Assume that the velocity of the dipping layer at 1 sec drops 15% from 4000m/s to 3400m/s before monitor surveying. Figure 16 shows the new velocity model used for generation of synthetic monitor survey data.

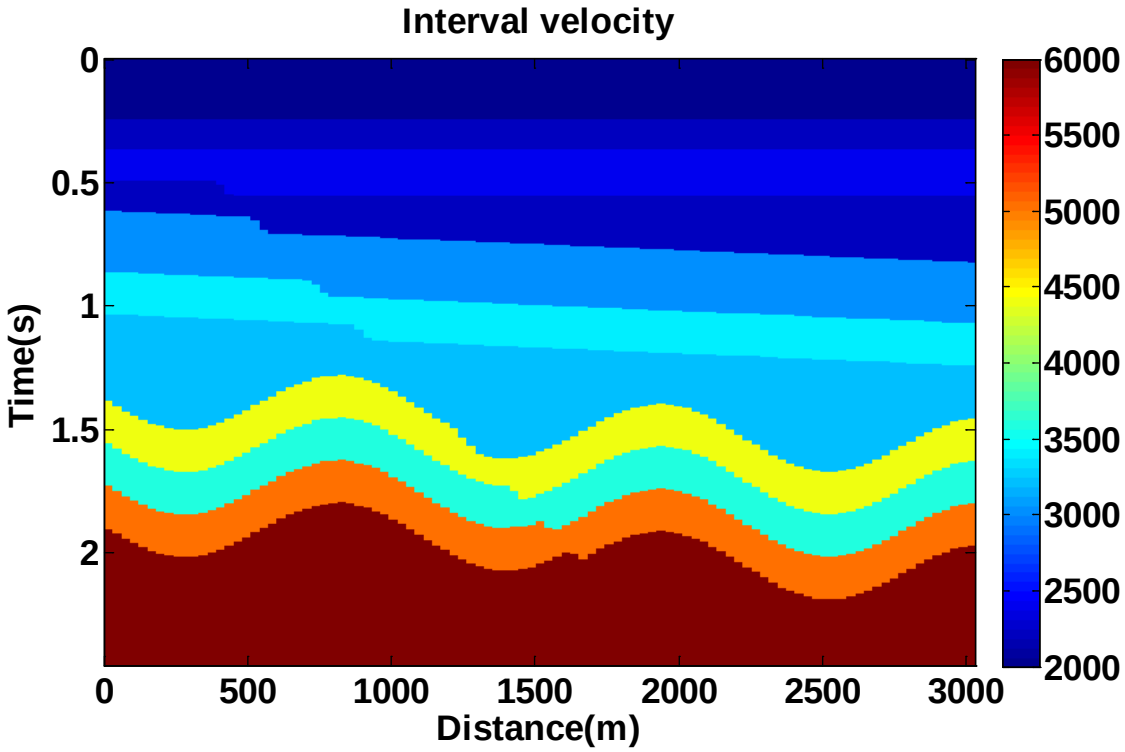

FIG. 16. Velocity model used in monitor survey.

Data are produced by baseline and monitor surveys with the corresponding velocity models. After adding 1% random noise, data are migrated. Figure 17a shows the difference between migration images of the baseline and monitor survey. The resulting time lapse image shows the difference in reflectivity due to velocity change. Since the only change in the velocity model is the dipping layer at 1sec, all other events below 1.3sec are migration artifacts and not changes in the model parameters. Figure 17b shows the difference between LSPSM images. Comparison between two images shows that LSPSM time lapse image has higher resolution than the migration time lapse image and artifacts in migration time lapse image are attenuated.

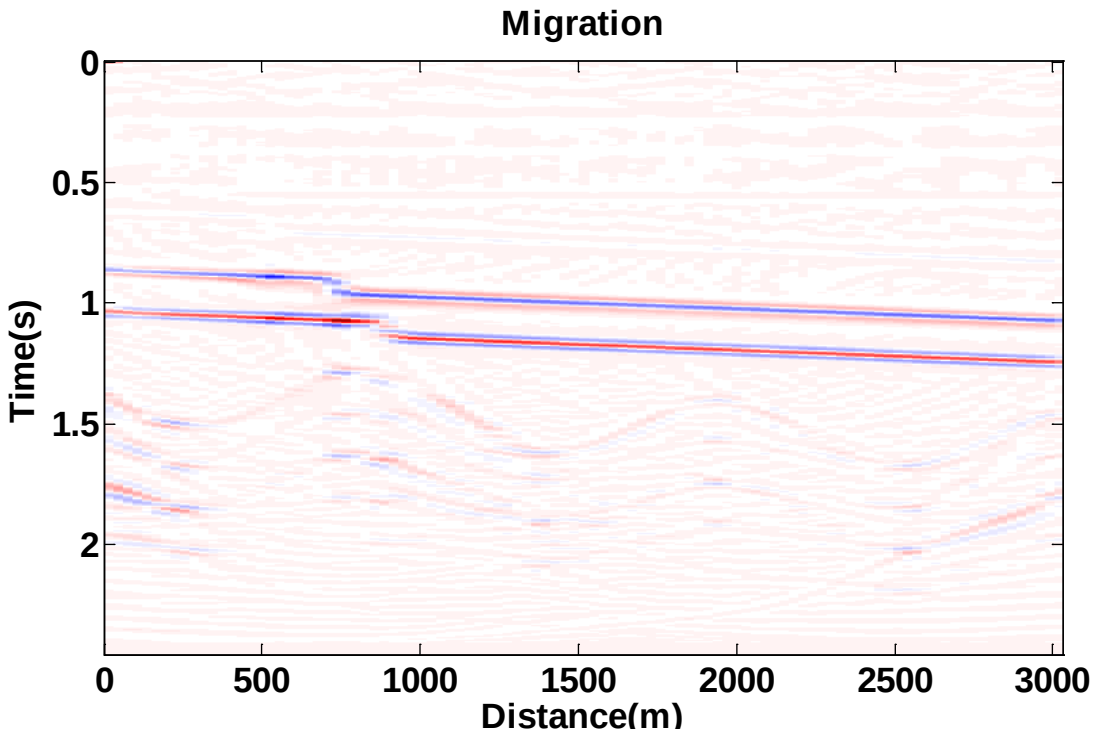

a)

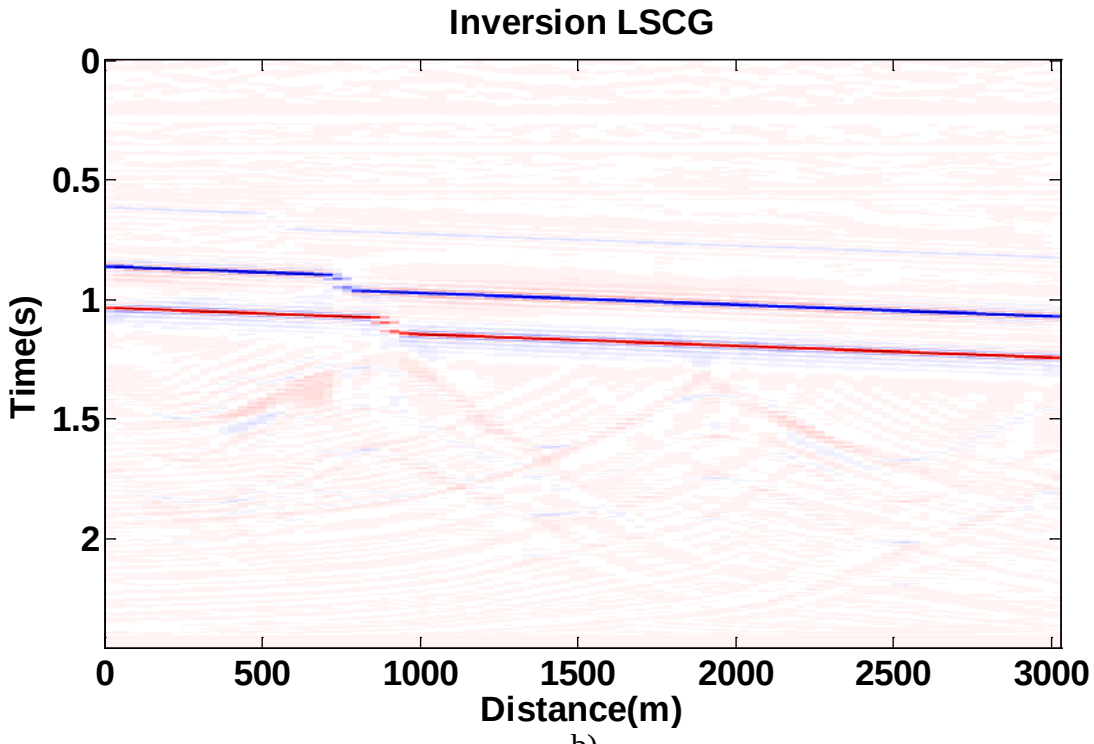

b)

FIG. 17. Migration (a) and LSPSM (b) time lapse image.

Figure 18 shows baseline and monitor survey data for a CMP at 2000m. Figure 18c shows the difference between baseline and monitor surveys. Events above depth of 1sec are cancelled. Due to time shift below 1sec, events are not comparable below the depth of change in the model parameters.

Figure 19 shows the reconstructed baseline data, monitor data, and their difference. LSPSM which 20 LSCG iterations is used for data reconstruction. However, the velocity model of the baseline survey is used in forward modeling and data reconstruction of monitor survey data. The difference panel in Figure 19c can be considered as the difference between baseline and monitor data (Figure 18c) when the effect of time shift is removed from data below the velocity change area.

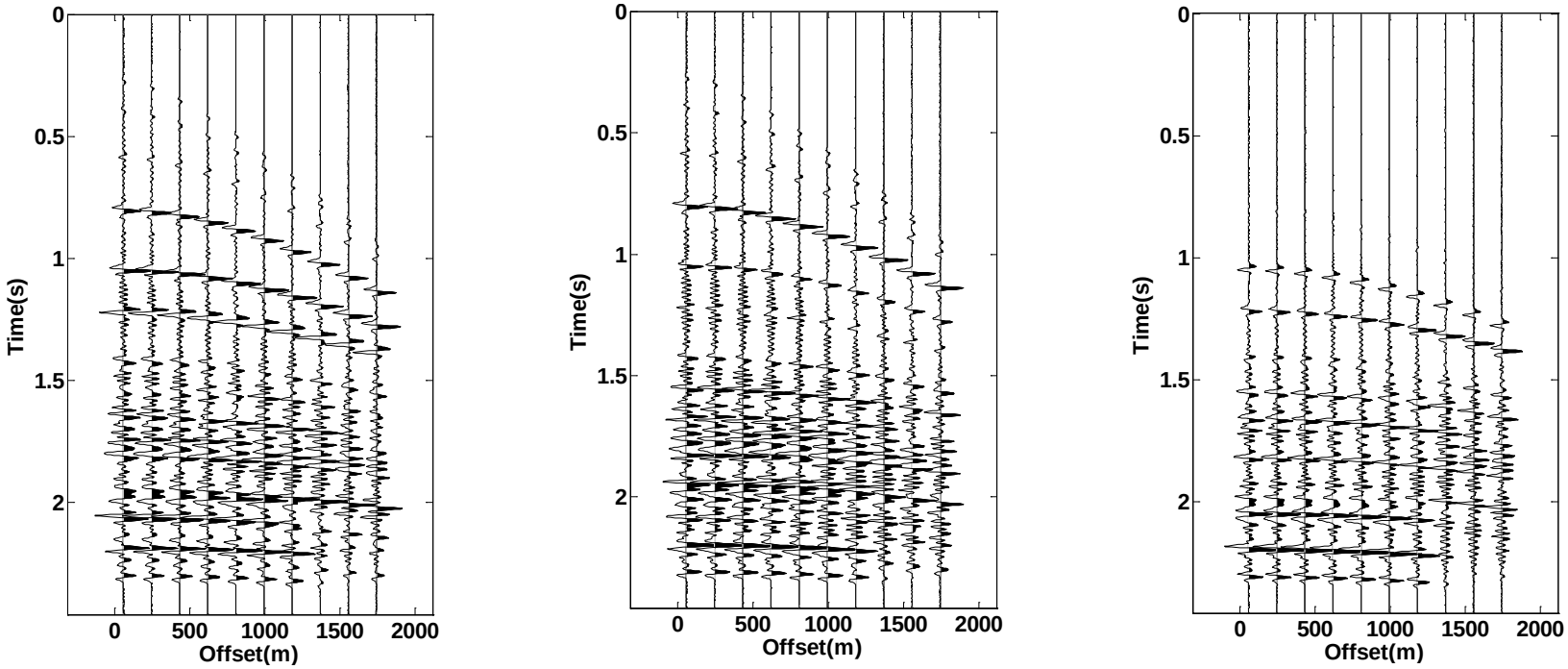

a) b) c)

FIG. 18. CMP gathers from baseline (a) and monitor surveys (b), and their difference (c).

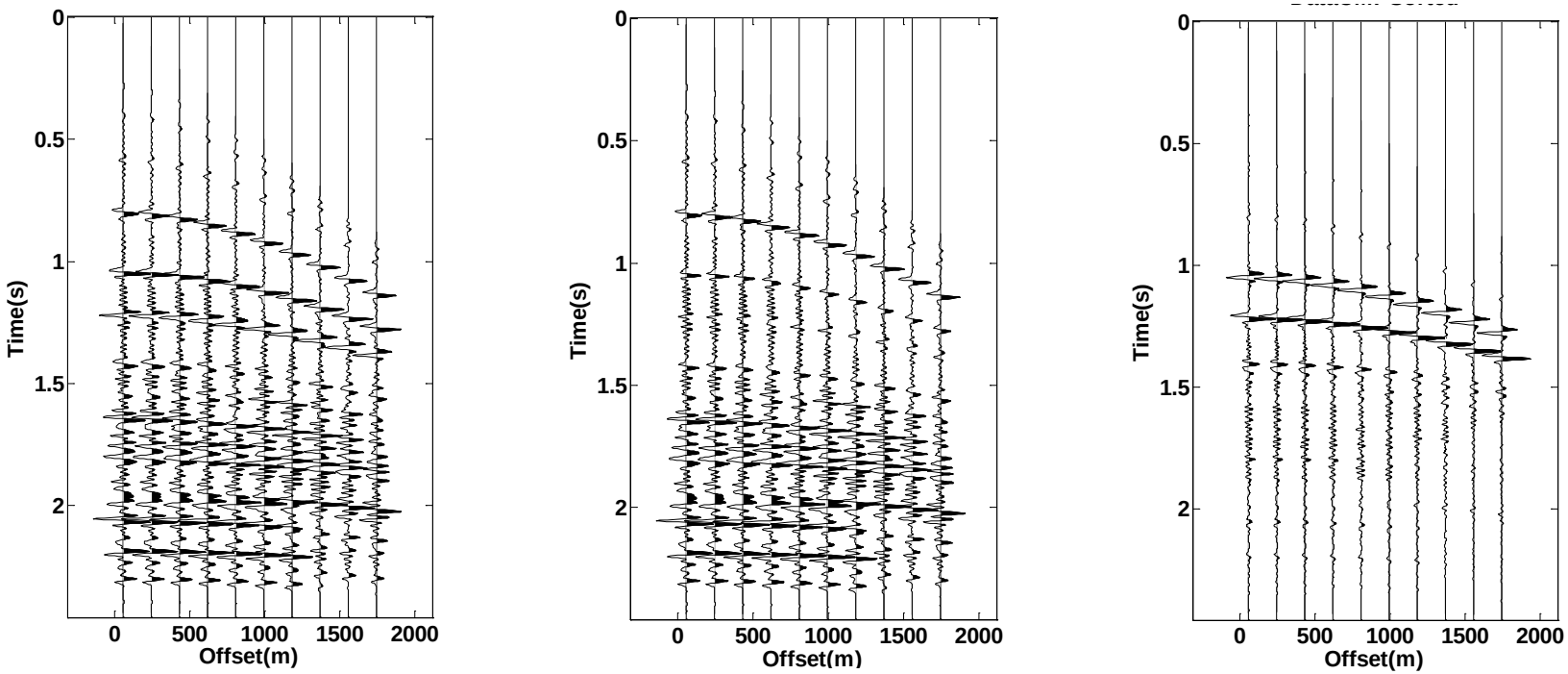

a) b) c)

FIG. 19. Reconstructed CMP gathers from baseline (a) and monitor surveys (b), and their difference (c).

JOINT INVERSION OF TIME LAPSE DATA BY LSPSM

The advantages of using LSPSM and data reconstruction methods for time lapse studies of seismic data is shown in previous sections. We performed a separate LSPSM for each (baseline and monitor) dataset ignoring presence of the other dataset at a time. In this section, we show the simultaneous inversion of the baseline and monitor survey data.

Ayeni and Biondi (2010) performed least squares joint inversion of time lapse data using two related formulation. Their first formulation was simultaneous inversion of multiple images, referred to as "Regularized Joint inversion of Multiple Images" (RJMI) and second was inversion for baseline and the difference (time lapse) images, referred to as "Regularized Joint inversion for Image Differences" (RJID). The RJMI method returns baseline and monitor images and the output of RJID method is the baseline image and difference between baseline and monitor image. Ayeni and Biondi (2010) used approximations to the wave equation least squares Hessian matrices to perform their inversion in the image domain. Implementing least squares in the image domain enabled them to target-orient their equation and reduce the high cost of the wave equation least squares migration.

In this study, we use Kirchhoff LSPSM for the joint inversion of time lapse data which is cheaper than the wave equation least squares inversion. To do so, with the same methodology that Ayeni and Biondi (2010) implemented, we combine the two cost functions for the separate damped LSPSM/inversion of the baseline survey

$$J_0(\boldsymbol{m_0}) = \|\boldsymbol{G_0 m_0} - \boldsymbol{d_0}\|^2 + \mu_0^2 \|\boldsymbol{m_0}\|^2 \tag{11}$$

and monitor survey

$$J_1(\boldsymbol{m_1}) = \|\boldsymbol{G_1 m_1} - \boldsymbol{d_1}\|^2 + \mu_1^2 \|\boldsymbol{m_1}\|^2 , \tag{12}$$

into the Multiple Image Joint Inversion (MIJI) cost function as

$$J_{MIJI}(\boldsymbol{m_0}, \boldsymbol{m_1}) = \left\| \begin{bmatrix} \boldsymbol{G_0} & \boldsymbol{0} \\ \boldsymbol{0} & \boldsymbol{G_1} \end{bmatrix} \begin{bmatrix} \boldsymbol{m_0} \\ \boldsymbol{m_1} \end{bmatrix} - \begin{bmatrix} \boldsymbol{d_0} \\ \boldsymbol{d_1} \end{bmatrix} \right\|^2 + \left\| \begin{bmatrix} \mu_0 & 0 \\ 0 & \mu_1 \end{bmatrix} \begin{bmatrix} \boldsymbol{m_0} \\ \boldsymbol{m_1} \end{bmatrix} \right\|^2 . \tag{13}$$

This is similar to RJMI. The time lapse image can be computed by

$$\boldsymbol{\Delta m_{miji}} = \boldsymbol{m_{miji1}} - \boldsymbol{m_{miji0}}, \tag{14}$$

where $\boldsymbol{m_{miji0}}$ and $\boldsymbol{m_{miji1}}$ are the baseline and monitor survey reflectivity images resulted from MIJI, respectively.

Alternatively, joint inversion can be performed to achieve time lapse image, $\boldsymbol{\Delta m}$, directly by minimizing the Image Difference Joint Inversion (IDJI) cost function as

$$J_{IDJI}(\boldsymbol{m_0}, \boldsymbol{\Delta m}) = \left\| \begin{bmatrix} \boldsymbol{G_0} & \boldsymbol{0} \\ \boldsymbol{G_1} & \boldsymbol{G_1} \end{bmatrix} \begin{bmatrix} \boldsymbol{m_0} \\ \boldsymbol{\Delta m} \end{bmatrix} - \begin{bmatrix} \boldsymbol{d_0} \\ \boldsymbol{d_1} \end{bmatrix} \right\|^2 + \left\| \begin{bmatrix} \mu_0 & 0 \\ 0 & \mu_1 \end{bmatrix} \begin{bmatrix} \boldsymbol{m_0} \\ \boldsymbol{\Delta m} \end{bmatrix} \right\|^2 . \tag{15}$$

This is similar to RJID formulation.

I used LSCG to minimize these cost functions. As an example, ignoring regularization terms, $\mu_0 = \mu_1 = 0$, a simplified LSCG algorithm to minimize $J_{IDJI}$is shown in Table 1. As seen in this table, each iteration in this LSCG algorithm includes performing two migrations and two modelings. Therefore, each iteration is at least four times more expensive than one time migration of the baseline survey data. My experience shows that the convergence of the above mentioned joint inversion algorithms are slower than the convergence of separates LSPSM in the previous section.

I performed MIJI and IDJI on the synthetic example in first section of this report. Results are shown after 50 iterations in the LSCG. Figure 20 and Figure 21 show the resulted from MIJI of baseline and monitor survey reflectivity images, respectively. The time lapse image is shown in Figure 22. Figure 23 and Figure 24 show the baseline and time lapse images resulted from IDJI, respectively.

Comparison between Figure 22 and Figure 24 shows higher resolution time lapse is achieved by MIJI. This can be due to the difference between structure of the Hessian matrices in the MIJI and IDJI. IDJI forward modeling matrix is 50% denser than the MIJI matrix. MIJI matrix is symmetric where IDJI is not. Therefore, MIJI is better solved by the LSCG method.

Comparison between separate LSPSM of time lapse image (Figure 17a) and MIJI (Figure 22) shows that the MIJI has slightly less artifacts in the resulted time lapse image than the time image from separate LSPSM. However, It is necessary to mention that time lapse image of MIJI is achieved after 50 LSCG iterations which is equal to 200 migration cost where the separate LSPSM image is achieved after 20 iteration on each datasets which is equal to the cost of 80 migration.

Table 1. LSCG algorithm for solving image difference joint inversion equation.

$\boldsymbol{m}_0 =$ an initial guess or $\boldsymbol{m}_0 = \mathbf{0}$

$\boldsymbol{\Delta m} = \mathbf{0}$

$\boldsymbol{s}_0 = \boldsymbol{d_0} - \boldsymbol{G_0 m}_0$

$\boldsymbol{s}_1 = \boldsymbol{d1} - \boldsymbol{G_1}(\boldsymbol{m}_0 + \boldsymbol{\Delta m})$

$\boldsymbol{r}_1 = \boldsymbol{G}_1^T \boldsymbol{s}_1$

$\boldsymbol{r}_0 = \boldsymbol{G}_0^T \boldsymbol{s}_0 + \mathbf{r_1}$

$\boldsymbol{p}_0 = \boldsymbol{r}_0$

$\boldsymbol{p}_1 = \boldsymbol{r}_1$

$\boldsymbol{q}_0 = \boldsymbol{G_0 p}_0$

$\boldsymbol{q}_1 = \boldsymbol{G_1}(\boldsymbol{p_0} + \boldsymbol{p_1})$

for $i = 0$: iterations limit

$$\alpha_{i+1} = \frac{\boldsymbol{r_{0i}} . \boldsymbol{r_{0i}} + \boldsymbol{r_{1i}} . \boldsymbol{r_{1i}}}{\boldsymbol{q_{0i}} . \boldsymbol{q_{0i}} + \boldsymbol{q_{1i}} . \boldsymbol{q_{1i}}}$$

$$\boldsymbol{m_{0}}_{i+1} = \boldsymbol{m_{0}}_{i} + \alpha_{i+1} \boldsymbol{p_{0}}_{i}$$

$$\boldsymbol{\Delta m}_{i+1} = \boldsymbol{\Delta m}_{i} + \alpha_{i+1} \boldsymbol{p_{1}}_{i}$$

$$\boldsymbol{s_{0}}_{i+1} = \boldsymbol{s_{0}}_{i} - \alpha_{i+1} \boldsymbol{q_{0}}_{i}$$

$$\boldsymbol{s_{1}}_{i+1} = \boldsymbol{s_{1}}_{i} - \alpha_{i+1} \boldsymbol{q_{1}}_{i}$$

$$\boldsymbol{r_{1}}_{i+1} = \boldsymbol{G_1^T s_{1}}_{i+1} \qquad \rightsquigarrow$$

$$\boldsymbol{r_{0}}_{i+1} = \boldsymbol{G_0^T s}_{i+1} + \boldsymbol{r_{1}}_{i+1} \qquad \rightsquigarrow$$

$$\beta_{i+1} = \frac{\boldsymbol{r_{0}}_{i+1} . \boldsymbol{r_{0}}_{i+1} + \boldsymbol{r_{1}}_{i+1} . \boldsymbol{r_{1}}_{i+1}}{\boldsymbol{r_{1}}_{i} . \boldsymbol{r_{1}}_{i}}$$

$$\boldsymbol{p_{0}}_{i+1} = \boldsymbol{r_{0}}_{i+1} + \beta_{i+1} \boldsymbol{p_{0}}_{i}$$

$$\boldsymbol{p_{1}}_{i+1} = \boldsymbol{r_{1}}_{i+1} + \beta_{i+1} \boldsymbol{p_{1}}_{i}$$

$$\boldsymbol{q_{0}}_{i+1} = \boldsymbol{G_0 p_{0}}_{i+1} \qquad \leftsquigarrow$$

$$\boldsymbol{q_{1}}_{i+1} = \boldsymbol{G_1}(\boldsymbol{p_{0}}_{i+1} + \boldsymbol{p_{1}}_{i+1}) \qquad \leftsquigarrow$$

endfor

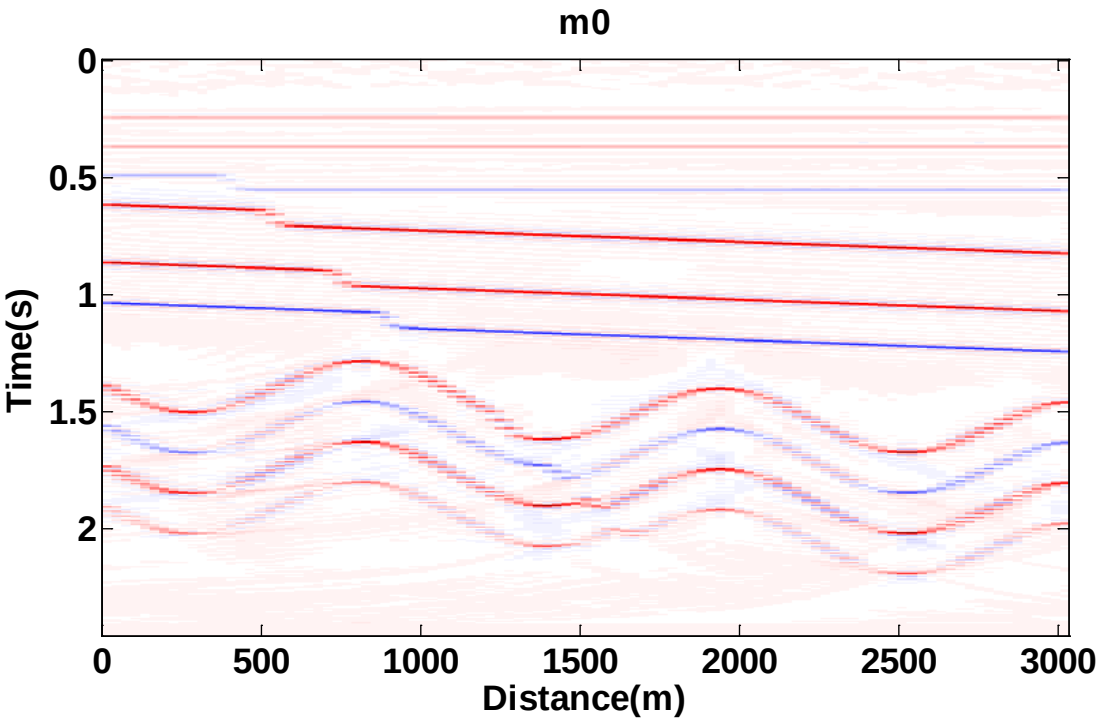

FIG. 20. Reflectivity of baseline survey achieved by MIJI.

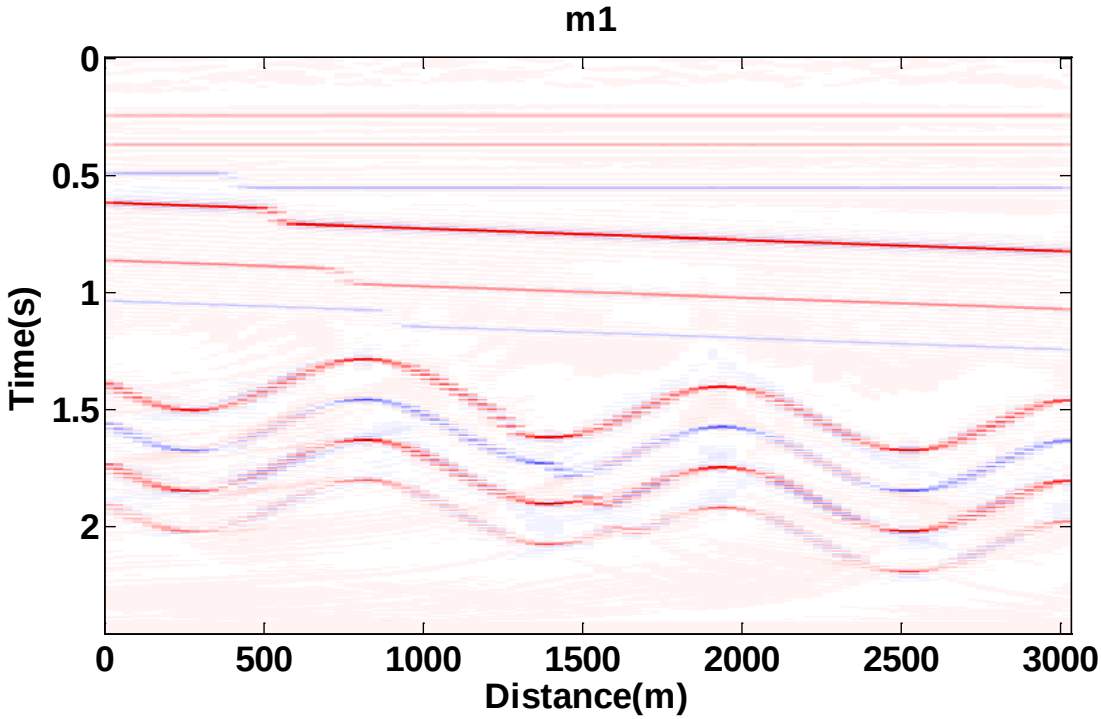

FIG. 21. Reflectivity of monitor survey achieved by MIJI.

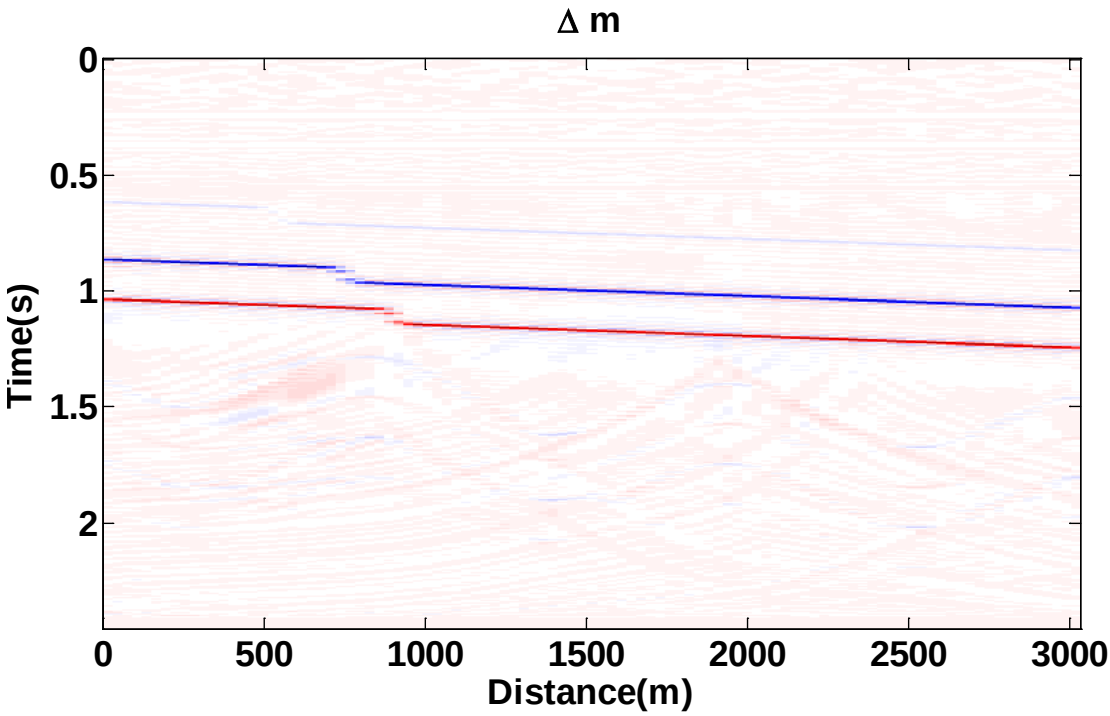

FIG. 22. Difference between reflectivity of baseline and monitor surveys by MIJI.

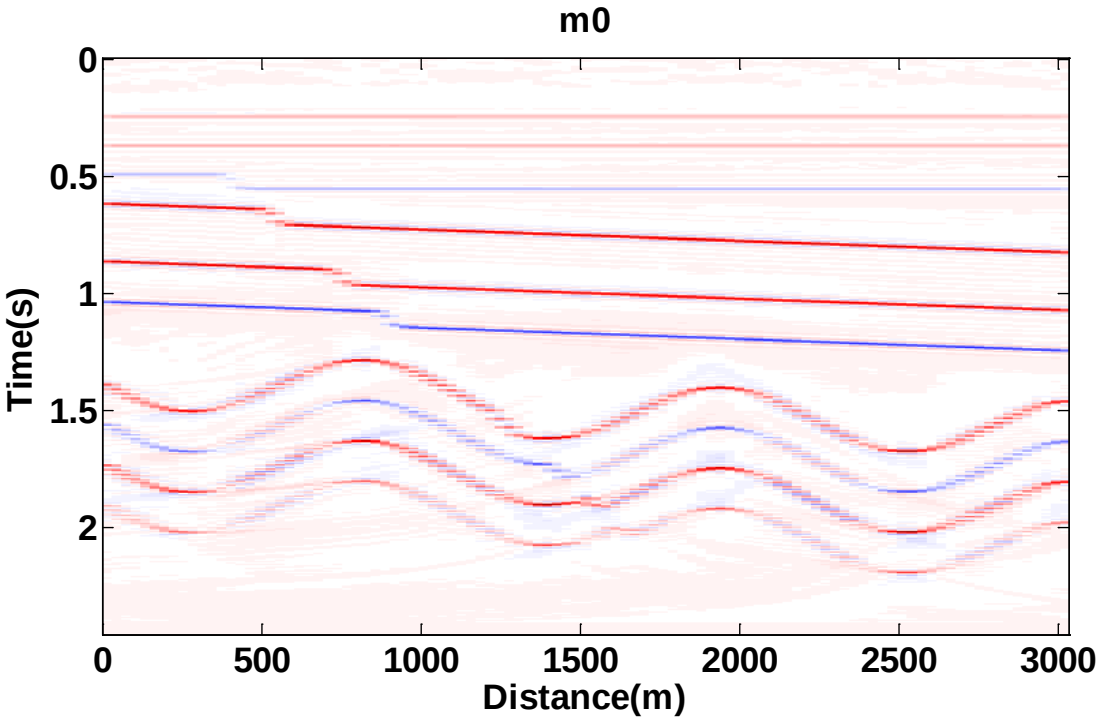

FIG. 23. Reflectivity of baseline survey achieved by IDJI.

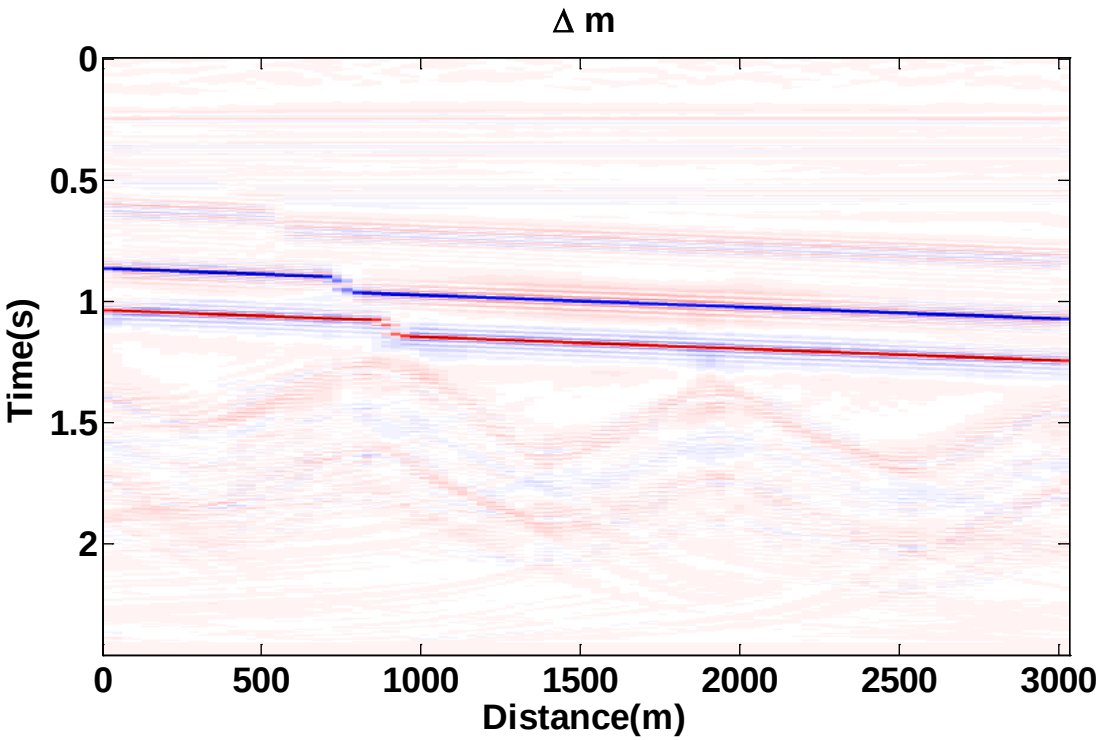

FIG. 24. Time lapse image from reflectivity by IDJI.

The formulation for the joint inversion of baseline and monitor survey data can be extended to the joint inversion of baseline and several monitor surveys.

For example if the subsurface reflectivity model changes from $\boldsymbol{m_1}$ to $\boldsymbol{m_2 = m1 + \Delta m_1}$ between the two monitor surveys, the second monitor survey data, $\boldsymbol{d_2}$, can be expressed by

$$\boldsymbol{d_2 = G_2\, m_2 = G_2(m_1 + \Delta m_1) = G_2(m_0 + \Delta m + \Delta m_1)}, \qquad (16)$$

where $\boldsymbol{G_2}$is the forward modeling operator of second monitor survey.

Then, the corresponding join inversion methods can retrieve the $\boldsymbol{m_0}$, $\boldsymbol{m_1}$, and $\boldsymbol{m_2}$ via MIJI or $\boldsymbol{m_0}$, $\boldsymbol{\Delta m}$, and $\boldsymbol{\Delta m_1}$via IDJI by minimizing the following cost functions

$$J_{MIJI}(\boldsymbol{m_0}, \boldsymbol{m_1}, \boldsymbol{m_2}) = \left\| \begin{bmatrix} \boldsymbol{G_0} & \boldsymbol{0} & \boldsymbol{0} \\ \boldsymbol{0} & \boldsymbol{G_1} & \boldsymbol{0} \\ \boldsymbol{0} & \boldsymbol{0} & \boldsymbol{G_2} \end{bmatrix} \begin{bmatrix} \boldsymbol{m_0} \\ \boldsymbol{m_1} \\ \boldsymbol{m_2} \end{bmatrix} - \begin{bmatrix} \boldsymbol{d_0} \\ \boldsymbol{d_1} \\ \boldsymbol{d_2} \end{bmatrix} \right\|^2 + \left\| \begin{bmatrix} \mu_0 & 0 & 0 \\ 0 & \mu_1 & 0 \\ 0 & 0 & \mu_2 \end{bmatrix} \begin{bmatrix} \boldsymbol{m_0} \\ \boldsymbol{m_1} \\ \boldsymbol{m_2} \end{bmatrix} \right\|^2 . \qquad (17)$$

and

$$J_{IDJI}(\boldsymbol{m_0}, \boldsymbol{\Delta m}, \boldsymbol{\Delta m_1}) = \left\| \begin{bmatrix} \boldsymbol{G_0} & \boldsymbol{0} & \boldsymbol{0} \\ \boldsymbol{G_1} & \boldsymbol{G_1} & \boldsymbol{0} \\ \boldsymbol{G_2} & \boldsymbol{G_2} & \boldsymbol{G_2} \end{bmatrix} \begin{bmatrix} \boldsymbol{m_0} \\ \boldsymbol{\Delta m} \\ \boldsymbol{\Delta m_1} \end{bmatrix} - \begin{bmatrix} \boldsymbol{d_0} \\ \boldsymbol{d_1} \\ \boldsymbol{d_2} \end{bmatrix} \right\|^2 + \left\| \begin{bmatrix} \mu_0 & 0 & 0 \\ 0 & \mu_1 & 0 \\ 0 & 0 & \mu_2 \end{bmatrix} \begin{bmatrix} \boldsymbol{m_0} \\ \boldsymbol{\Delta m} \\ \boldsymbol{\Delta m_1} \end{bmatrix} \right\|^2 . \qquad (18)$$

CONCLUSION

The ability of separate and joint LSPSM/inversion of time lapse data is discussed in this report. Assuming similarity of the acquisition instruments, environmental noise, near surface effects, and processing flows and parameters for both baseline and monitor surveys, difference in acquisition geometries leaves different artifacts at the migration images. These artifacts create unreal change of reflectivity in the time lapse image. It is shown how LSPSM of both, baseline and monitor, datasets can attenuate acquisition footprints and create reliable time lapse images. The reconstructed data from two surveys makes the prestack time lapse studies more feasible. Formulations of the joint inversion of time lapse data to invert for the baseline image and time lapse image by LSCG method are derived.

It is important to mention that this is an expensive procedure. Each iteration of the joint inversion cost more than four times performing migration. Other correction such as removing the near surface effects, multiple attenuation must be performed before inverting the data.

ACKNOWLEDGMENTS

Authors wish to acknowledge the sponsors of CREWES project for their continuing support. They also appreciate Kevin Hall and Rolf Maier in the CREWES project.

REFERENCES

Ayeni, G., and B. Biondi, 2010, Target-oriented joint least-squares migration/inversion of time-lapse seismic data sets: Geophysics, 75, R62-R73.

Greaves, R. J., and T. J., Fulp, 1987, Three-dimensional seismic monitoring of an enhanced oil recovery process: Geophysics, 52, 1175-1187.

Lumley, D. E., 2001, The next wave in reservoir monitoring: The instrumented oil field: The Leading Edge, 20, 640-648.

Nemeth, T., C. Wu, and G. T. Schuster, 1999, Least-squares migration of incomplete reflection data: Geophysics, 64, no. 1, 208-221.

Rickett, J. E., and D. E. Lumley, 2001, Cross-equalization data processing for time-lapse seismic reservoir monitoring: A case study from the Gulf of Mexico: Geophysics, 66, 1015-1025.

Vedanti, N., and M. K. Sen, 2009, Seismic inversion tracks in situ combustion: A case study from Balol oil field. India: Geophysics, 74, 103-112.